

# Small-Mass Asymptotics of Massive Point Vortex Dynamics in Bose–Einstein Condensates

Tomoki Ohsawa<sup>1</sup> and Andrea Richaud<sup>2</sup>

<sup>1</sup>Department of Mathematical Sciences, The University of Texas at Dallas, 800 W Campbell Rd, Richardson, TX 75080-3021

<sup>2</sup>Departament de Física, Universitat Politècnica de Catalunya, Campus Nord B4-B5, E-08034 Barcelona, Spain

March 28, 2025

## Abstract

We perform an asymptotic analysis of the massive point vortex dynamics in Bose–Einstein condensates in the small-mass limit  $\varepsilon \rightarrow 0$ . We show that the orthogonal projection of the massive dynamics to a certain subspace  $\mathcal{K}$  (called kinematic subspace) in the phase space yields the standard massless vortex dynamics or the Kirchhoff equations. We show that the massless dynamics is the zeroth-order approximation to the massive equation as  $\varepsilon \rightarrow 0$ , and also derive a first-order correction to the zeroth-order massless dynamics. The massive dynamics near  $\mathcal{K}$  is well approximated by the corresponding massless dynamics. In fact, our main result proves that the massive dynamics starting in  $\mathcal{K}$  stays  $O(\varepsilon)$ -close to  $\mathcal{K}$  for short time. On the other hand, the massive dynamics starting outside  $\mathcal{K}$  exhibits an oscillatory initial layer due to its inertia and deviates significantly from the massless dynamics. We also perform an asymptotic analysis with a rescaled time to derive the inner approximation to capture the initial layer. The 0th-order inner equations are exactly solvable, and the 1st-order inner equations can be solved by quadrature. The combined inner approximation captures the initial oscillatory layer of the massive dynamics.

## 1 Introduction

The standard description of vortex motion in superfluids has conventionally treated vortices as massless topological defects, leading to the familiar point-vortex (or Kirchhoff) equations [35, 38]. However, in many real experimental settings, the cores of quantum vortices in superfluids are actually filled, either intentionally or unintentionally, by massive particles, so that the vortices acquire a small but nonzero effective inertial mass. Examples include tracer atoms introduced in superfluid liquid helium to visualize vortex lines [7, 23, 43], quasiparticle bound states in both fermionic [6, 34, 56, 60, 62] and bosonic [62] superfluids even at zero temperature. Moreover, experimental conditions inherently involve non-zero temperatures, leading to the presence of thermal atoms localized in vortex cores, both in atomic Bose–Einstein condensates (BECs) [24] and in Fermi superfluids (see Refs. [6, 56] and references therein). Additionally, in two-component BECs, atoms of one species can become localized within the vortex cores of the other species [18, 20, 47, 52, 53]. These examples highlight that neglecting vortex mass can overlook crucial properties of the dynamics, motivating a shift from the purely massless approximation to massive point-vortex models [18, 28, 31, 52–54], which are essential for describing realistic quantum fluids.

In fact, even if the vortex mass is relatively small compared to that of the whole superfluid, it can significantly alter the dynamics of vortices by introducing non-trivial inertial effects. As a result, one observes oscillatory phenomena [18, 28, 31, 53, 54] and collisions [55] absent within the purely massless descriptions. These issues are central also in systems involving multicomponent [5, 64] or strongly coupled superfluids, where vortex-bound structures can display unusual stability or instability properties [1, 2, 36, 69]. In fermionic superfluids [26, 32, 41, 60], for instance, inertial corrections are deeply connected to the presence of the so-called normal component localized at the vortex core (see the recent Ref. [56] and references therein). Other examples include vortex–bright-soliton complexes emerging in two-component condensates [1, 29, 37, 57, 58, 67]. Moreover, the influence of vortex mass is expected to be relevant in BECs subject to coherent couplings [14, 15], dipolar interactions [50], or optical-lattice modulations [3], and for polar-core spin vortices in ferromagnetic spin-1 BECs [66, 68], underscoring its broad conceptual and experimental importance.

From a mathematical point of view, the introduction of a small core mass introduces *singular perturbation* to the original Kirchhoff equations. In particular, we would like to see how the small mass introduced to the system affects the dynamics, in comparison to the massless (Kirchhoff) dynamics, using techniques from singular perturbation theory [30, 45, 46].

In this paper, we perform an asymptotic analysis of the massive point-vortex system in two-component BECs, focusing on how the traditional massless description is recovered at the zeroth order as well as unveiling the next-order contributions that capture transient inertial features.

Our results clarify, via asymptotic analysis, when and how the vortex mass becomes appreciable and how it affects vortex trajectories. Specifically, we shall identify a subspace  $\mathcal{K}$  in the phase space in which the massive dynamics is approximated well by the massless dynamics; hence  $\mathcal{K}$  is called the *kinematic subspace* here in the sense that the massive dynamics (2nd-order system on the configuration space) approximately behaves like the massless/kinematic system (1st-order system on the configuration space). Intuitively, this implies that the massive solution starting in  $\mathcal{K}$  stays close to  $\mathcal{K}$  for a certain amount of time. Our main result is a rigorous proof of it.

We also numerically observe that solutions starting outside  $\mathcal{K}$  deviate significantly from the massless solution. In particular, massive solutions starting outside  $\mathcal{K}$  exhibit oscillatory initial layers due to its inertia; this is absent in the massless dynamics. We perform an asymptotic analysis of this initial layer with a time scale adjusted to the fast oscillations, and show that the zeroth-order initial layer dynamics is explicitly solvable, and the first-order correction is solvable by quadrature. Numerical results show that the analytical solutions capture the initial layer of the massive dynamics, giving the inner solution (or the temporal boundary layer solution) to the massive dynamics.

## 2 Massive Point Vortex Dynamics

### 2.1 Lagrangian for $N$ Massive Vortices in Two-Component BEC

We consider a two-component Bose–Einstein Condensate in the immiscible regime, confined in a quasi-two-dimensional disk trap of radius  $R$ , with hard-wall boundary conditions. The majority component, labeled “ $a$ ”, hosts  $N$  quantized vortices of topological charges  $\{q_j \in \{\pm 1\}\}_{j=1}^N$  while the minority component, labeled “ $b$ ”, occupies the vortex cores. The total masses of the two components are given by  $M_a := N_a m_a$  and  $M_b := N_b m_b$ , where  $N_a$  and  $N_b$  denote the total number of atoms in each component, and  $m_a$  and  $m_b$  are their respective atomic masses. In the absence of component  $b$ , the vortices in component  $a$  follow the standard first-order dynamics characteristic of massless point vortices or the Kirchhoff equations [35]. However, in the immiscible regime, the

minority component  $b$  becomes localized within the vortex cores, effectively endowing the vortices with mass. Assuming that the total mass  $M_b$  is evenly distributed among the  $N$  vortices, each vortex acquires an effective mass of  $M_b/N$  [52, 53].

Let  $\mathbf{r}_j = (x_j, y_j)$  be the position of the  $j$ -th vortex, and  $r_j := |\mathbf{r}_j| = (\mathbf{r}_j \cdot \mathbf{r}_j)^{1/2}$  be its length. We shall also use  $\mathbf{r} := (\mathbf{r}_1, \dots, \mathbf{r}_N)$  for short and similarly  $\dot{\mathbf{r}} := (\dot{\mathbf{r}}_1, \dots, \dot{\mathbf{r}}_N)$  etc. According to Richaud et al. [52, 53], the Lagrangian for the  $N$  massive vortices reads

$$L(\mathbf{r}, \dot{\mathbf{r}}) := \sum_{j=1}^N \left( \frac{M_b}{2N} \dot{\mathbf{r}}_j^2 + \pi n_a \hbar q_j (\dot{\mathbf{r}}_j \times \mathbf{r}_j) \cdot \hat{\mathbf{z}} \right) - E(\mathbf{r}), \quad (1)$$

where  $n_a$  is the two-dimensional number density, the cross product  $\mathbf{a} \times \mathbf{b}$  of two planar vectors  $\mathbf{a}, \mathbf{b} \in \mathbb{R}^2$  are taken by attaching zero as the third components to both, and is seen as a vector in  $\mathbb{R}^2$  or  $\mathbb{R}^3$  depending on the context,  $\hat{\mathbf{z}} := (0, 0, 1)$ , and  $E$  is the energy of the standard (massless) vortices

$$E(\mathbf{r}) := \frac{\pi n_a \hbar^2}{m_a} \sum_{j=1}^N \ln \left( 1 - \frac{r_j^2}{R^2} \right) + \frac{\pi n_a \hbar^2}{m_a} \sum_{1 \leq j < k \leq N} q_j q_k \ln \left( \frac{R^2 - 2\mathbf{r}_j \cdot \mathbf{r}_k + r_j^2 r_k^2 / R^2}{r_j^2 - 2\mathbf{r}_j \cdot \mathbf{r}_k + r_k^2} \right). \quad (2)$$

It is useful to express Lagrangian (1) in rescaled non-dimensional variables. We set the disk radius  $R$  as the unit of length,  $m_a R^2 / \hbar$  as the unit of time, and  $\pi n_a \hbar^2 / m_a$  as the unit of energy. In this natural units, which we adopt henceforth, the Lagrangian takes the form:

$$L(\mathbf{r}, \dot{\mathbf{r}}) := \sum_{j=1}^N \left( \frac{\varepsilon}{2} \dot{\mathbf{r}}_j^2 + q_j (\dot{\mathbf{r}}_j \times \mathbf{r}_j) \cdot \hat{\mathbf{z}} \right) - E(\mathbf{r}), \quad (3)$$

where the only effective parameter  $\varepsilon$  is defined as

$$\varepsilon := \frac{M_b / M_a}{N},$$

and the potential-energy term reads

$$E(\mathbf{r}) := \sum_{j=1}^N \ln(1 - r_j^2) + \sum_{1 \leq j < k \leq N} q_j q_k \ln \left( \frac{1 - 2\mathbf{r}_j \cdot \mathbf{r}_k + r_j^2 r_k^2}{|\mathbf{r}_j - \mathbf{r}_k|^2} \right).$$

*Remark 1.* Due to the assumed confining potential, strictly speaking, one must restrict the positions of the vortices to the open unit disk, i.e.,

$$\mathbf{r}_j \in \mathbb{B}_1(0) := \{\mathbf{x} \in \mathbb{R}^2 \mid |\mathbf{x}| < 1\} \quad \text{for } 1 \leq j \leq N,$$

and also have to avoid collision points—those points with  $\mathbf{r}_i = \mathbf{r}_j$  with  $i \neq j$ —so that the above energy function  $E$  is defined. However, in what follows, we shall ignore these issues for simplicity unless otherwise stated, because the geometric consideration to follow is simpler to describe by assuming  $\mathbf{r} \in \mathbb{R}^{2N}$ . Alternatively, one may extend the definition of  $E$  to the entire  $\mathbb{R}^{2N}$  by assigning values to  $E$  outside  $(\mathbb{B}_1(0))^N$  and collision points. Either way, one may then consider the dynamics only in the subset of  $\mathbb{R}^{2N}$  in which the original  $E$  makes sense.

We are mainly interested in the asymptotic behavior of the massive point vortices in the small-mass limit, i.e.,  $0 < \varepsilon \ll 1$ . This regime is particularly relevant from a physical perspective, as quantum vortices in real superfluid systems are rarely, if ever, truly massless, and often are equipped with small masses, as explained in the Introduction.

## 2.2 Hamiltonian Formulation

Using the Lagrangian (3), the Legendre transformation is defined via the momenta  $\mathbf{p} := (\mathbf{p}_1, \dots, \mathbf{p}_N)$  with

$$\mathbf{p}_j := \frac{\partial L}{\partial \dot{\mathbf{r}}_j} = \varepsilon \dot{\mathbf{r}}_j + q_j(\mathbf{r}_j \times \hat{\mathbf{z}}), \quad (4)$$

giving

$$\dot{\mathbf{r}}_j = \frac{1}{\varepsilon}(\mathbf{p}_j - q_j(\mathbf{r}_j \times \hat{\mathbf{z}})).$$

Hence we may define the Hamiltonian

$$\begin{aligned} H(\mathbf{r}, \mathbf{p}) &:= \sum_{j=1}^N \mathbf{p}_j \cdot \dot{\mathbf{r}}_j - L(\mathbf{r}, \dot{\mathbf{r}}) \\ &= \frac{1}{2\varepsilon} \sum_{j=1}^N (\mathbf{p}_j - q_j(\mathbf{r}_j \times \hat{\mathbf{z}}))^2 + E(\mathbf{r}) \\ &= \frac{1}{2\varepsilon} \sum_{j=1}^N (p_j^2 - 2q_j(\mathbf{r}_j \times \hat{\mathbf{z}}) \cdot \mathbf{p}_j + q_j^2 r_j^2) + E(\mathbf{r}). \end{aligned} \quad (5)$$

Then Hamilton's equations

$$\dot{\mathbf{r}}_j = \frac{\partial H}{\partial \mathbf{p}_j}, \quad \dot{\mathbf{p}}_j = -\frac{\partial H}{\partial \mathbf{r}_j}$$

yield

$$\varepsilon \dot{\mathbf{r}}_j = \mathbf{p}_j - q_j(\mathbf{r}_j \times \hat{\mathbf{z}}), \quad \varepsilon \dot{\mathbf{p}}_j = q_j(\hat{\mathbf{z}} \times \mathbf{p}_j) - q_j^2 \mathbf{r}_j - \varepsilon \nabla_j E(\mathbf{r}),$$

where  $\nabla_j$  stands for  $\partial/\partial \mathbf{r}_j$ , i.e., the gradient with respect to  $\mathbf{r}_j$ .

For the sake of brevity, let us define

$$J := \begin{bmatrix} 0 & 1 \\ -1 & 0 \end{bmatrix} \text{ so that } J\mathbf{a} = \mathbf{a} \times \hat{\mathbf{z}} \quad \forall \mathbf{a} \in \mathbb{R}^2. \quad (6)$$

Then we have

$$\varepsilon \dot{\mathbf{r}}_j = \mathbf{p}_j - q_j J \mathbf{r}_j, \quad \varepsilon \dot{\mathbf{p}}_j = -q_j J(\mathbf{p}_j - q_j J \mathbf{r}_j) - \varepsilon \nabla_j E(\mathbf{r}). \quad (7)$$

One may eliminate  $\mathbf{p}_j$  from above to obtain the following second-order differential equations

$$\varepsilon \ddot{\mathbf{r}}_j + 2q_j J \dot{\mathbf{r}}_j = -\nabla_j E(\mathbf{r}), \quad (8)$$

which are nothing but the Euler–Lagrange equations for the Lagrangian  $L$  in (3). Clearly these systems are singularly perturbed systems when  $\varepsilon \ll 1$ .

The Hamiltonian formulation is particularly useful in highlighting the drastic effect of introducing a core mass. In the massless case, in fact,  $x_j$  is canonically conjugate to  $q_j y_j$ , i.e., the massless  $N$ -vortex system is a Hamiltonian system with  $N$  degrees of freedom (associated to a  $2N$ -dimensional phase space). However, in the massive case, the system gains  $2N$  independent momenta, doubling the dimension of the associated phase space to  $4N$ . Despite this increase, the number of conserved quantities, typically arising from the symmetry properties of the superfluid domain, remains unchanged. As a result, the introduction of a core mass can break integrability. A clear example is the two-vortex system in a disk. In the massless limit, there are only two degrees of freedom, matching the number of conserved quantities (energy and angular momentum)

and therefore ensuring integrability [8]. In contrast, the massive case has four degrees of freedom, while still preserving only two conserved quantities. Hence the system may be chaotic unless hidden invariants exist. This distinction is particularly relevant for long-time dynamics, where small differences in initial conditions, such as identical positions but slightly different velocities, may be exponentially amplified, leading to drastically different final states.

### 3 Geometry of the Kinematic Approximation

#### 3.1 The Kinematic Approximation and the Kirchhoff Equation

Taking the limit  $\varepsilon \rightarrow 0$  in (8), one obtains

$$2q_j J \dot{\mathbf{r}}_j = -\nabla_j E(\mathbf{r}) \iff \begin{cases} 2q_j \dot{x}_j = \frac{\partial E}{\partial y_j}, \\ 2q_j \dot{y}_j = -\frac{\partial E}{\partial x_j}. \end{cases} \quad (9)$$

These are nothing but the Kirchhoff equations for massless vortices, and give the natural kinematic or massless approximation to the massive point vortex equations (8).

According to these equations, each vortex moves with the local superfluid velocity at its position, determined by the superposition of all velocity fields induced by all the other vortices in the system. To be more specific, the velocity field generated at a point  $\mathbf{r}$  by the  $j$ -th vortex, located at  $\mathbf{r}_j$  and having topological charge  $q_j$ , is  $\mathbf{v}(\mathbf{r}) = q_j \hat{\mathbf{z}} \times (\mathbf{r} - \mathbf{r}_j) / |\mathbf{r} - \mathbf{r}_j|^2$ . A vortex hence moves with the velocity obtained by summing the contributions from all other vortices (except itself), be they physical vortices or image vortices ensuing from the presence of boundaries. This framework is well established in classical hydrodynamics, where Euler's equations describe the evolution of an inviscid and incompressible fluid [8, 35].

#### 3.2 Kinematic Subspace $\mathcal{K}$

We would like to give a geometric interpretation of the above kinematic approximation in the limit  $\varepsilon \rightarrow 0$ . First notice that taking the limit  $\varepsilon \rightarrow 0$  in (7) gives

$$\mathbf{p}_j = q_j J \mathbf{r}_j \iff \begin{bmatrix} \xi_j \\ \eta_j \end{bmatrix} = q_j \begin{bmatrix} y_j \\ -x_j \end{bmatrix} \quad (10)$$

where we wrote  $\mathbf{p}_j = (\xi_j, \eta_j)$ . One may interpret the above constraints as the natural kinematic constraints in the massless limit  $\varepsilon \rightarrow 0$  in the definition (4) of the momentum  $\mathbf{p}$  (or the Legendre transformation).

Defining the cotangent bundle—the phase space for the Hamiltonian system (7)—as

$$T^*\mathbb{R}^{2N} = \{(\mathbf{r}, \mathbf{p}) \in \mathbb{R}^{2N} \times \mathbb{R}^{2N} \mid \mathbf{p} \in T_{\mathbf{r}}^*\mathbb{R}^{2N} \cong \mathbb{R}^{2N}\} \cong \mathbb{R}^{4N},$$

the above kinematic constraints (10) give rise to the following *kinematic subspace*:

$$\mathcal{K} := \{(\mathbf{r}, \mathbf{p}) \in T^*\mathbb{R}^{2N} \mid \mathbf{p}_j = q_j J \mathbf{r}_j \text{ for } 1 \leq j \leq N\}.$$

Clearly,  $\mathcal{K}$  is an  $2N$ -dimensional subspace of  $T^*\mathbb{R}^{2N} \cong \mathbb{R}^{4N}$ . One also sees that  $\mathbf{r} = (\mathbf{r}_1, \dots, \mathbf{r}_N) \in \mathbb{R}^{2N}$  gives coordinates for  $\mathcal{K}$  via the following map (see Figure 1):

$$\varphi: \mathbb{R}^{2N} \rightarrow \mathcal{K}; \quad \mathbf{r} = (\mathbf{r}_1, \dots, \mathbf{r}_N) \mapsto \varphi(\mathbf{r}) := (\mathbf{r}_1, \dots, \mathbf{r}_N, q_1 J \mathbf{r}_1, \dots, q_N J \mathbf{r}_N), \quad (11)$$

and hence also giving the identification

$$\mathcal{K} = \varphi(\mathbb{R}^{2N}) \cong \mathbb{R}^{2N}.$$

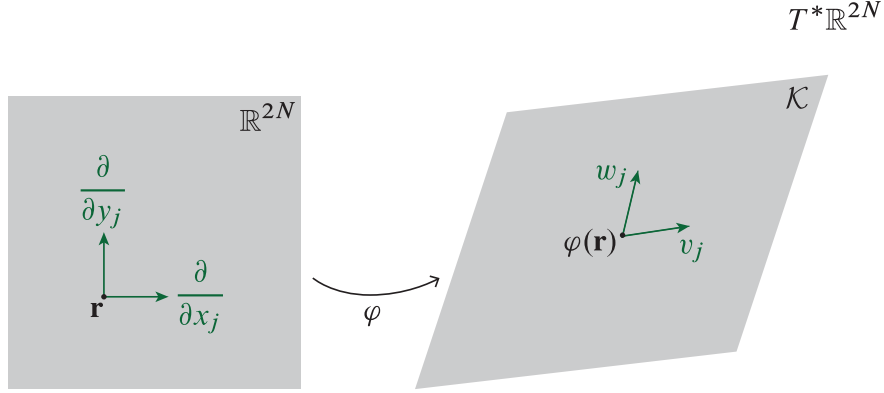


Figure 1: Subspace  $\mathcal{K}$  and tangent vectors  $v_j, w_j \in T_{\varphi(\mathbf{r})}\mathcal{K}$  forming a basis  $\{v_j, w_j\}_{j=1}^N$  for  $T_{\varphi(\mathbf{r})}\mathcal{K}$ . Note that, strictly speaking, the tangent vectors in the figure live in tangent spaces of  $\mathbb{R}^{2N}$  and  $\mathcal{K}$  but are drawn in the base spaces for simplicity.

The Jacobian of  $\varphi$  is given by

$$D\varphi(\mathbf{r}) = \begin{bmatrix} I & 0 \\ 0 & I \\ 0 & D_q \\ -D_q & 0 \end{bmatrix} \quad \text{with} \quad D_q := \text{diag}(q_1, \dots, q_N).$$

Thus the tangent vectors  $\frac{\partial}{\partial x_j}$  and  $\frac{\partial}{\partial y_j}$  in  $T_{\mathbf{r}}\mathbb{R}^{2N}$  are mapped to the following vectors in  $T_{\varphi(\mathbf{r})}\mathcal{K}$  by  $D\varphi$  as follows:

$$v_j := D\varphi(\mathbf{r})\frac{\partial}{\partial x_j} = \frac{\partial}{\partial x_j} - q_j \frac{\partial}{\partial \eta_j}, \quad w_j := D\varphi(\mathbf{r})\frac{\partial}{\partial y_j} = \frac{\partial}{\partial y_j} + q_j \frac{\partial}{\partial \xi_j}, \quad (12)$$

which are written as tangent vectors in  $T_{\varphi(\mathbf{r})}T^*\mathbb{R}^{2N} = \text{span}\{\frac{\partial}{\partial x_j}, \frac{\partial}{\partial y_j}, \frac{\partial}{\partial \xi_j}, \frac{\partial}{\partial \eta_j}\}_{j=1}^N$ ; see Figure 1. As a result, we have the following basis for the tangent space  $T_{\varphi(\mathbf{r})}\mathcal{K}$ :

$$\left\{ v_j := \frac{\partial}{\partial x_j} - q_j \frac{\partial}{\partial \eta_j}, w_j := \frac{\partial}{\partial y_j} + q_j \frac{\partial}{\partial \xi_j} \right\}_{j=1}^N. \quad (13)$$

### 3.3 Geometric Interpretation of the Kinematic Approximation

We shall show that the Kirchhoff equation (9) is a natural Hamiltonian system induced in the kinematic subspace  $\mathcal{K} \subset T^*\mathbb{R}^{2N}$  by the Hamiltonian system (7) for massive point vortices. To see this, first note that the standard symplectic form on  $T^*\mathbb{R}^{2N}$  is given by

$$\Omega := \mathbf{d}\mathbf{r}_j \wedge \mathbf{d}\mathbf{p}_j = \mathbf{d}x_j \wedge \mathbf{d}\xi_j + \mathbf{d}y_j \wedge \mathbf{d}\eta_j, \quad (14)$$

where  $\mathbf{d}$  stands for the exterior derivative, and the summation convention is assumed on  $j$ ; its matrix representation is the  $4N \times 4N$  matrix

$$\mathbb{J} := \begin{bmatrix} 0 & I \\ -I & 0 \end{bmatrix}$$

with  $I$  being the  $2N \times 2N$  identity matrix; so we have  $\Omega(v, w) = v^T \mathbb{J} w$  with all  $v, w \in T_{(\mathbf{r}, \mathbf{p})} T^* \mathbb{R}^{2N} \cong \mathbb{R}^{4N}$ .

Writing vector field  $X_H$  on  $T^* \mathbb{R}^{2N}$  as

$$X_H = \dot{\mathbf{r}}_j \frac{\partial}{\partial \mathbf{r}_j} + \dot{\mathbf{p}}_j \frac{\partial}{\partial \mathbf{p}_j} = \dot{x}_j \frac{\partial}{\partial x_j} + \dot{y}_j \frac{\partial}{\partial y_j} + \dot{\xi}_j \frac{\partial}{\partial \xi_j} + \dot{\eta}_j \frac{\partial}{\partial \eta_j},$$

the Hamiltonian system (7) is then equivalent to

$$\mathbf{i}_{X_H} \Omega = \mathbf{d}H,$$

where  $\mathbf{i}$  stands for the interior product (or insertion/contraction) of a vector field with a differential form. More concretely, one may think of  $X_H$  and  $\nabla H$  as column vectors in  $\mathbb{R}^{4N}$  so that the above system becomes equivalent to

$$X_H^T \mathbb{J} = (\nabla H)^T \iff X_H = \mathbb{J} \nabla H.$$

As a result, we have

$$X_H = \frac{1}{\varepsilon} (\mathbf{p}_j - q_j J \mathbf{r}_j) \frac{\partial}{\partial \mathbf{r}_j} - \left( \frac{1}{\varepsilon} q_j J (\mathbf{p}_j - q_j J \mathbf{r}_j) + \nabla_j E(\mathbf{r}) \right) \frac{\partial}{\partial \mathbf{p}_j} \quad (15)$$

With an abuse of notation, we may change the codomain of  $\varphi$  to  $T^* \mathbb{R}^{2N}$  and consider

$$\varphi: \mathbb{R}^{2N} \rightarrow T^* \mathbb{R}^{2N}.$$

Then  $\varphi$  gives an embedding of  $\mathbb{R}^{2N}$  into  $T^* \mathbb{R}^{2N}$  as the subspace  $\mathcal{K} = \varphi(\mathbb{R}^{2N})$ . Let us consider the pull-back of the symplectic form  $\Omega$  to  $\mathcal{K} \cong \mathbb{R}^{2N}$  by  $\varphi$ :

$$\omega := \varphi^* \Omega = 2 \sum_{j=1}^N q_j \mathbf{d}x_j \wedge \mathbf{d}y_j,$$

where  $\varphi^*$  stands for the pull-back by  $\varphi$ , and we did *not* use the summation convention here; its matrix representation is

$$\mathbb{K} := (D\varphi(\mathbf{r}))^T \mathbb{J} D\varphi(\mathbf{r}) = 2 \begin{bmatrix} 0 & \mathbf{D}_q \\ -\mathbf{D}_q & 0 \end{bmatrix}.$$

Similarly, the pull-back of the Hamiltonian  $H$  to  $\mathcal{K} \cong \mathbb{R}^{2N}$  by  $\varphi$  gives

$$(\varphi^* H)(\mathbf{r}) = H \circ \varphi(\mathbf{r}) = E(\mathbf{r}),$$

where the last equality follows by using the expression (5) and the kinematic constraints (10) defining  $\mathcal{K}$ .

Writing vector field  $X_E$  on  $\mathcal{K} \cong \mathbb{R}^{2N}$  as

$$X_E = \dot{\mathbf{r}}_j \frac{\partial}{\partial \mathbf{r}_j} = \dot{x}_j \frac{\partial}{\partial x_j} + \dot{y}_j \frac{\partial}{\partial y_j},$$

we have a Hamiltonian system defined on  $\mathbb{R}^{2N}$  as

$$\mathbf{i}_{X_E} \omega = \mathbf{d}E$$

in terms of the symplectic form  $\omega$  and Hamiltonian  $E$  naturally induced on  $\mathbb{R}^{2N}$  as the pull-backs by  $\varphi$  of  $\Omega$  and  $H$ ; see Figure 2. Seeing  $X_E$  and  $\nabla E$  as column vectors in  $\mathbb{R}^{2N}$ , the above system is equivalent to

$$X_E^T \mathbb{K} = (\nabla E)^T \iff X_E = (\mathbb{K}^T)^{-1} \nabla E = \frac{1}{2} \begin{bmatrix} 0 & D_q \\ -D_q & 0 \end{bmatrix} \nabla E,$$

noting that  $q_j^{-1} = q_j$  because  $q_j = \pm 1$ ; as a result, we have

$$X_E(\mathbf{r}) = \frac{q_j}{2} \frac{\partial E}{\partial y_j} \frac{\partial}{\partial x_j} - \frac{q_j}{2} \frac{\partial E}{\partial x_j} \frac{\partial}{\partial y_j}, \quad (16)$$

which is the vector field defined by the Kirchhoff equation (9).

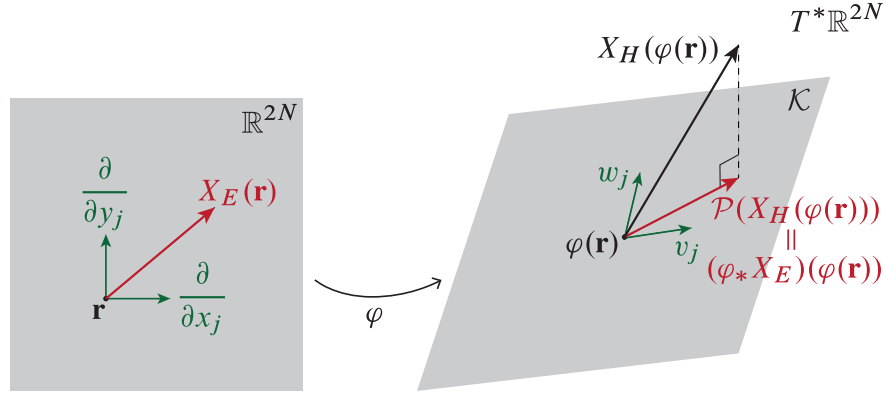


Figure 2: Orthogonally projecting  $X_H$ —the vector field defining the massive point vortex equation (7)—from the tangent space of  $T^*\mathbb{R}^{2N}$  to the tangent space of  $\mathcal{K}$  defines vector field  $\mathcal{P}(X_H)$  on  $\mathcal{K}$ ; this in turn corresponds via  $\varphi$  to vector field  $X_E$  on  $\mathbb{R}^{2N}$  defining the Kirchhoff equation (9).

### 3.4 Best Approximation Property

We shall show that the vector field  $X_E$  in  $\mathbb{R}^{2N}$ —more precisely its push-forward  $\varphi_* X_E$  on  $\mathcal{K}$ —is the best approximation to  $X_H$  in  $\mathcal{K}$  in the following sense (see also Figure 2):

**Proposition.** *Let  $g$  be the standard metric on  $T^*\mathbb{R}^{2N}$ , i.e.,*

$$g = dx_j \otimes dx_j + dy_j \otimes dy_j + d\xi_j \otimes d\xi_j + d\eta_j \otimes d\eta_j, \quad (17)$$

*and consider the Hamiltonian vector field  $X_H$  on  $T^*\mathbb{R}^{2N}$  (from (15)) for the massive vortex dynamics (7) as well as the Hamiltonian vector field  $X_E$  on  $\mathbb{R}^{2N}$  (from (16)) for the massless vortex dynamics (9). Then the orthogonal projection of  $X_H$  to the kinematic subspace  $\mathcal{K}$  is the push-forward  $\varphi_* X_E$  of  $X_E$  by  $\varphi: \mathbb{R}^{2N} \rightarrow \mathcal{K}$  defined in (11).*

*Proof.* First note that the basis (13) for  $T_{\varphi(\mathbf{r})}\mathcal{K}$  is an orthogonal basis with respect to the metric  $g$ :

$$g(v_i, v_j) = \delta_{ij} \|v_j\|^2, \quad g(w_i, w_j) = \delta_{ij} \|w_j\|^2, \quad g(v_i, w_j) = 0$$

with

$$\|v_j\| := g(v_j, v_j)^{1/2} = (1 + q_j^2)^{1/2} = \sqrt{2}, \quad \|w_j\| := g(w_j, w_j)^{1/2} = (1 + q_j^2)^{1/2} = \sqrt{2},$$



because we assume that  $q_j = \pm 1$ . We may then define the orthogonal projection

$$\mathcal{P}: T_{\varphi(\mathbf{r})}T^*\mathbb{R}^{2N} \rightarrow T_{\varphi(\mathbf{r})}\mathcal{K}; \quad V \mapsto \frac{g(v_j, V)}{\|v_j\|^2}v_j + \frac{g(w_j, V)}{\|w_j\|^2}w_j$$

using the summation convention on  $j$ .

Notice that  $X_H(\varphi(\mathbf{r}))$ , upon imposing the kinematic constraints (10) to the expression (15), takes the form

$$X_H(\varphi(\mathbf{r})) = -\frac{\partial E}{\partial x_j} \frac{\partial}{\partial \xi_j} - \frac{\partial E}{\partial y_j} \frac{\partial}{\partial \eta_j}$$

and thus, using the expressions for  $v_j$  and  $w_j$  from (13),

$$g(v_j, X_H(\varphi(\mathbf{r}))) = q_j \frac{\partial E}{\partial y_j}, \quad g(w_j, X_H(\varphi(\mathbf{r}))) = -q_j \frac{\partial E}{\partial x_j}$$

Hence we have the orthogonal projection of  $X_H(\varphi(\mathbf{r}))$  to  $T_{\varphi(\mathbf{r})}\mathcal{K}$  as follows:

$$\begin{aligned} \mathcal{P}(X_H(\varphi(\mathbf{r}))) &= \frac{g(v_j, X_H(\varphi(\mathbf{r})))}{\|v_j\|^2}v_j + \frac{g(w_j, X_H(\varphi(\mathbf{r})))}{\|w_j\|^2}w_j \\ &= \frac{q_j}{2} \frac{\partial E}{\partial y_j} v_j - \frac{q_j}{2} \frac{\partial E}{\partial x_j} w_j. \end{aligned}$$

Sending this vector field from  $\mathcal{K}$  to  $\mathbb{R}^{2N}$  using the correspondence  $v_j \leftrightarrow \frac{\partial}{\partial x_j}$  and  $w_j \leftrightarrow \frac{\partial}{\partial y_j}$  from (12) (i.e., the pull-back by  $\varphi$ ), we obtain the following vector field on  $\mathbb{R}^{2N}$ :

$$\frac{q_j}{2} \frac{\partial E}{\partial y_j} \frac{\partial}{\partial x_j} - \frac{q_j}{2} \frac{\partial E}{\partial x_j} \frac{\partial}{\partial y_j},$$

which is  $X_E(\mathbf{r})$ , defining the Kirchhoff equation (9):

$$\dot{x}_j = \frac{q_j}{2} \frac{\partial E}{\partial y_j}, \quad \dot{y}_j = -\frac{q_j}{2} \frac{\partial E}{\partial x_j},$$

where we again note that  $q_j^{-1} = q_j$  because  $q_j = \pm 1$ . □

We note that the above proposition is reminiscent of the so-called variational approximation or the Dirac–Frenkel–McLachlan variational principle [19, 22, 33, 39, 40, 42] that are often used in approximations of quantum dynamics.

### 3.5 Numerical Results: Massless vs. Massive near $\mathcal{K}$

Consider the vortex dipole case with the following parameters and initial conditions:

$$\begin{aligned} N &= 2, \quad q_1 = -1, \quad q_2 = 1, \quad \varepsilon = 0.01, \\ \mathbf{r}_1(0) &= (x_1(0), y_1(0)) = (0.6, 0.2), \quad \mathbf{r}_2(0) = (x_2(0), y_2(0)) = (-0.3, -0.4), \\ \mathbf{p}_1(0) &= q_1 J \mathbf{r}_1(0) = (-0.2, 0.6), \quad \mathbf{p}_2(0) = q_2 J \mathbf{r}_2(0) = (-0.4, 0.3). \end{aligned} \tag{18}$$

Notice that  $\mathbf{p}_j(0) = q_j J \mathbf{r}_j(0)$  so that  $(\mathbf{r}(0), \mathbf{p}(0))$  is in the kinematic subspace  $\mathcal{K}$ .

Figures 3 to 5 compare the massless solution of the Kirchhoff equation (9) with the massive solution of (7). We observe that the massless and massive solutions are very close to each other, although they slowly deviate from each other.

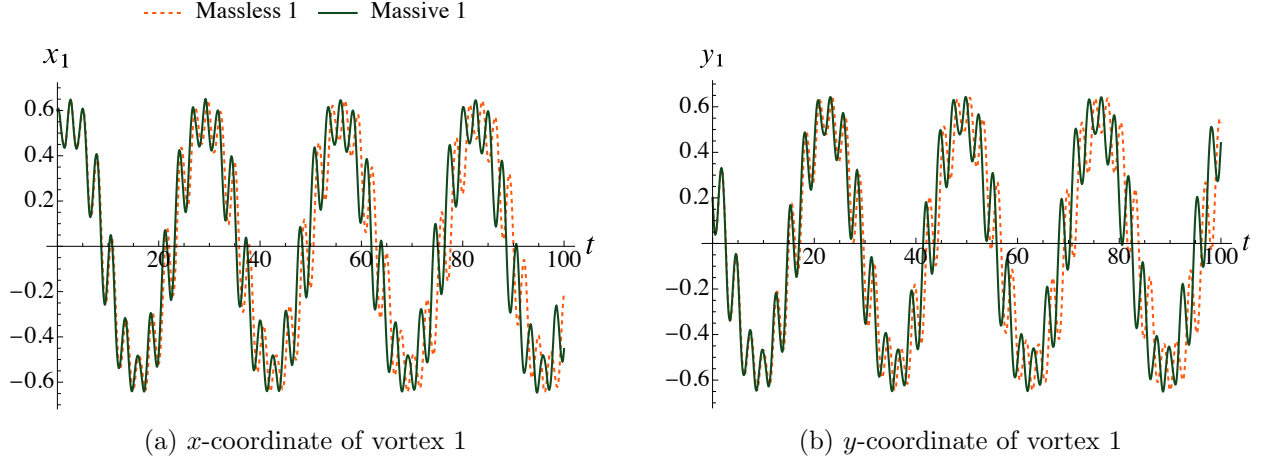


Figure 3: Massless and massive solutions of vortex 1 with parameters and initial conditions from (18) satisfying  $(\mathbf{r}(0), \mathbf{p}(0)) \in \mathcal{K}$ .

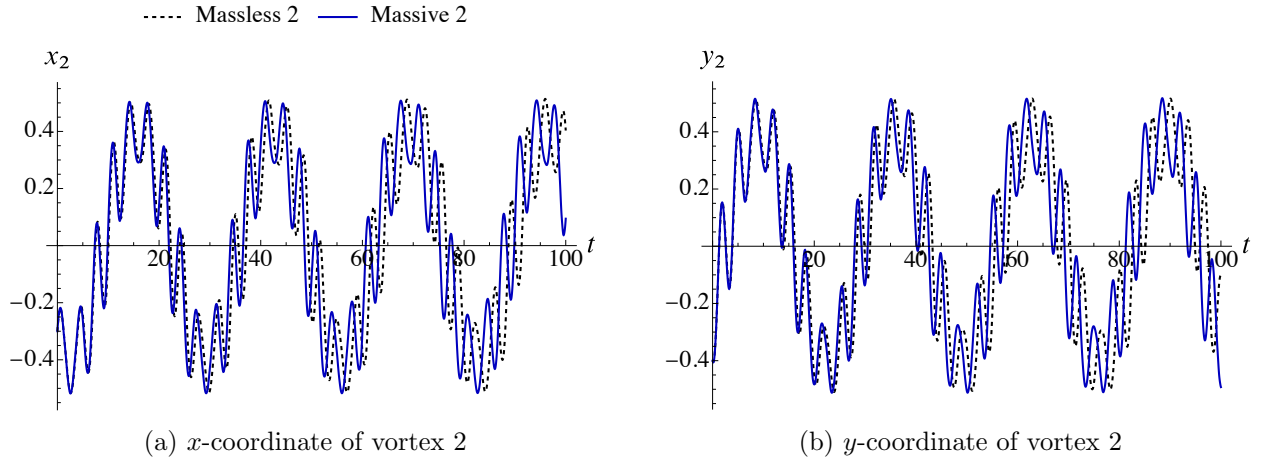


Figure 4: Massless and massive solutions of vortex 2 with parameters and initial conditions from (18) satisfying  $(\mathbf{r}(0), \mathbf{p}(0)) \in \mathcal{K}$ .

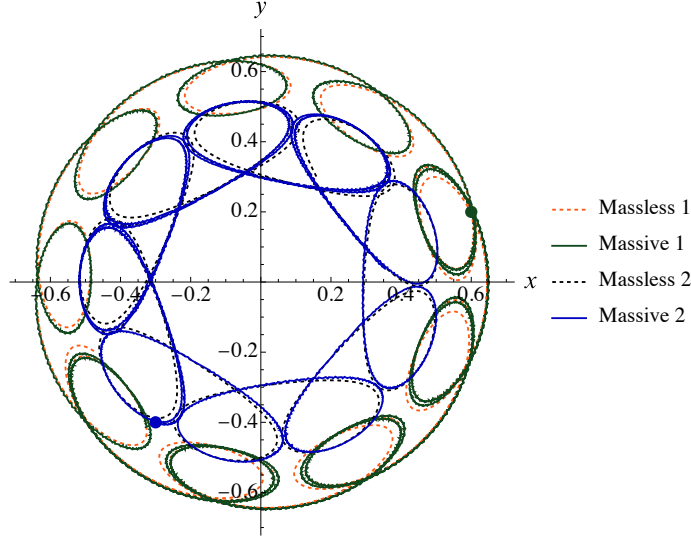


Figure 5: The trajectories of the massless and massive vortices on the  $(x, y)$ -plane for  $0 \leq t \leq 40$  with parameters and initial conditions (18).

### 3.6 Noether Invariants

The Hamiltonian (5) has the  $\text{SO}(2)$ -symmetry: For every planar rotation matrix  $\mathbf{R} \in \text{SO}(2)$ ,

$$H(\mathbf{R}\mathbf{r}_1, \dots, \mathbf{R}\mathbf{r}_N, \mathbf{R}\mathbf{p}_1, \dots, \mathbf{R}\mathbf{p}_N) = H(\mathbf{r}_1, \dots, \mathbf{r}_N, \mathbf{p}_1, \dots, \mathbf{p}_N).$$

The corresponding Noether invariant is the angular momentum

$$\ell(\mathbf{r}, \mathbf{p}) := \sum_{j=1}^N (\mathbf{r}_j \times \mathbf{p}_j) \cdot \hat{\mathbf{z}} = \sum_{j=1}^N (\mathbf{r}_j \times \hat{\mathbf{z}}) \cdot \mathbf{p}_j = \sum_{j=1}^N (J\mathbf{r}_j) \cdot \mathbf{p}_j$$

Its pull-back by  $\varphi$  (see (11)) gives

$$\mathcal{I}(\mathbf{r}) := (\varphi^* \ell)(\mathbf{r}) = \ell \circ \varphi(\mathbf{r}) = \sum_{j=1}^N (J\mathbf{r}_j) \cdot (q_j J\mathbf{r}_j) = \sum_{j=1}^N q_j r_j^2, \quad (19)$$

and this is the Noether invariant—the so-called angular impulse—of the Kirchhoff equation (9) corresponding to the  $\text{SO}(2)$ -symmetry.

Quantity (19) is closely related to the third component of the expectation value of the angular momentum of the  $N$ -vortex superfluid system, given in dimensionful units by  $L_{z,a} = \pi \hbar n_a \sum_{j=1}^N (R^2 - q_j r_j^2)$ , and in dimensionless units by  $L_{z,a} = \sum_{j=1}^N (1 - q_j r_j^2)$ . The angular impulse  $\mathcal{I}$  from above differs from this expression only by inessential additive and multiplicative constants. This formula can be derived by computing the expectation value  $L_{z,a} = \langle \psi_a | \hat{L}_z | \psi_a \rangle$  of the angular-momentum operator  $\hat{L}_z$  with respect to a suitably chosen trial wavefunction  $\psi_a$  capturing the main features of the state of component- $a$  BEC or of another quantum fluid (see Ref. [9] for further details). We note, in this regard, that the Lagrangian (3) is defined up to a total time derivative, allowing for different choices that lead to slight variations in the form of invariant (19). However, among these possible variations, differing only by additive and/or multiplicative constants, only one corresponds directly to the physically meaningful angular momentum of the system.

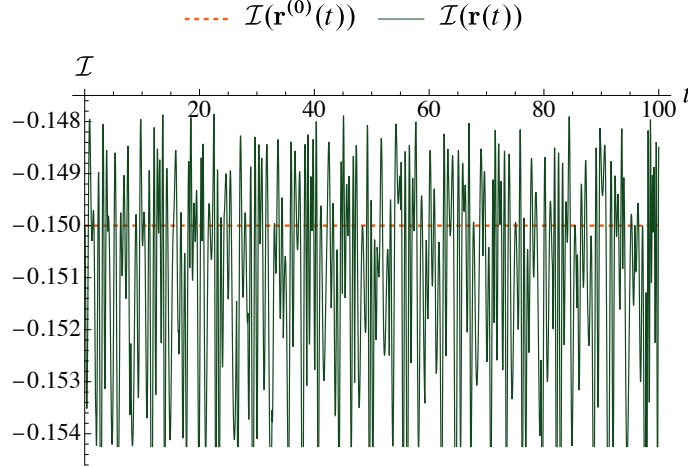


Figure 6: Time evolution of angular impulse  $\mathcal{I}$  (see (19)) along massless solution  $\mathbf{r}^{(0)}(t)$  and massive solution  $\mathbf{r}(t)$  with parameters and initial conditions from (18) satisfying  $(\mathbf{r}(0), \mathbf{p}(0)) \in \mathcal{K}$ .

Figure 6 shows the time evolution of the angular impulse  $\mathcal{I}$  from (19) along both the massless solution  $\mathbf{r}^{(0)}(t)$  and the massive solution  $\mathbf{r}(t)$  with parameters and initial conditions from (18) satisfying  $(\mathbf{r}(0), \mathbf{p}(0)) \in \mathcal{K}$ . Although  $\mathcal{I}$  is *not* an invariant of the massive equations (7), we see that  $\mathcal{I}(\mathbf{r}(t))$  is nearly conserved, oscillating near the actual conserved quantity  $\mathcal{I}(\mathbf{r}^{(0)}(t))$ . This result suggests that the invariant  $\mathcal{I}$  of the massless system nearly persists for the massive system when the massive solution stays close to  $\mathcal{K}$  when  $\varepsilon \ll 1$ .

## 4 Estimate of Deviation from the Kinematic Subspace $\mathcal{K}$

### 4.1 Deviation from $\mathcal{K}$

Let us write

$$\mathbf{g}_j(t) := \mathbf{p}_j(t) - q_j J \mathbf{r}_j(t) \in \mathbb{R}^2,$$

and also define

$$\mathbf{g}(t) := \begin{bmatrix} \mathbf{g}_1(t) \\ \vdots \\ \mathbf{g}_N(t) \end{bmatrix} \in \mathbb{R}^{2N}.$$

Then  $\|\mathbf{g}(t)\|$  gives an estimate of the deviation of the massive solution  $(\mathbf{r}(t), \mathbf{p}(t))$  from the kinematic subspace  $\mathcal{K}$ .

Figure 7 shows the time evolution of the deviation  $\|\mathbf{g}(t)\|$  for the numerical solution from the previous section. It suggests that if  $(\mathbf{r}(0), \mathbf{p}(0)) \in \mathcal{K}$ , that is,  $\|\mathbf{g}(0)\| = 0$ , then the deviation  $\|\mathbf{g}(t)\|$  for  $t > 0$  stays small for a certain amount of time.

### 4.2 Estimate of Deviation from $\mathcal{K}$

Notice in Figure 7 that  $\|\mathbf{g}(t)\|$  is  $O(\varepsilon)$ ; recall that  $\varepsilon = 0.01$  in this particular case. We shall prove that this is indeed the case as long as there are no collisions and the vortices do not hit the boundary—the unit circle in  $\mathbb{R}^2$ . To that end, first let  $\delta_1 \in (0, 1)$  and consider  $N$  copies of the

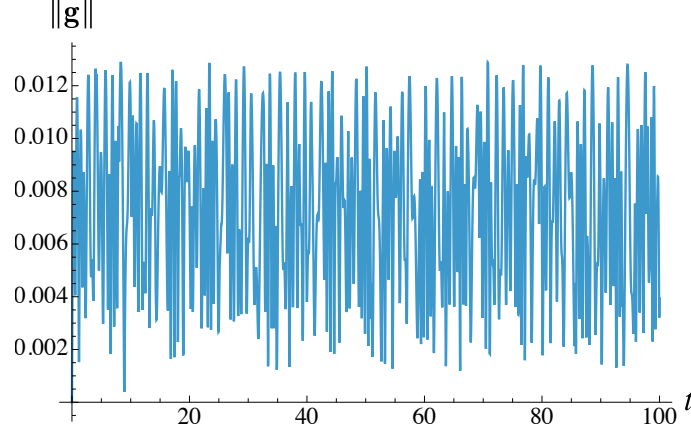


Figure 7: Time evolution of the deviation  $\|\mathbf{g}(t)\|$  massive solution  $\mathbf{r}(t)$  with parameters and initial conditions from (18) satisfying  $(\mathbf{r}(0), \mathbf{p}(0)) \in \mathcal{K}$ .

closed disk with radius  $1 - \delta_1$  centered at the origin:

$$\mathcal{D} := (\bar{\mathbb{B}}_{1-\delta_1}(0))^N = \{(\mathbf{r}_1, \dots, \mathbf{r}_N) \in \mathbb{R}^{2N} \mid |\mathbf{r}_i| \leq 1 - \delta_1 \text{ for } 1 \leq i \leq N\},$$

as well as the set of all possible collision points inside it:

$$\mathcal{C} := \{(\mathbf{r}_1, \dots, \mathbf{r}_N) \in \mathcal{D} \mid \mathbf{r}_i = \mathbf{r}_j \text{ with some } i \neq j\}.$$

Now define the distance from every point in  $\mathcal{D}$  to the set of collision points:

$$\rho: \mathcal{D} \rightarrow \mathbb{R}_{\geq 0}; \quad \rho(\mathbf{x}) := \inf_{\mathbf{y} \in \mathcal{C}} \|\mathbf{x} - \mathbf{y}\|,$$

where  $\|\cdot\|$  stands for the standard Euclidean norm on  $\mathbb{R}^{2N}$ . Let  $\delta_2 > 0$  and define

$$\mathcal{E}_{\delta_1, \delta_2} := \rho^{-1}([\delta_2, \infty)).$$

Then we see that  $\mathcal{E}_{\delta_1, \delta_2}$  is compact: Since  $\rho$  is continuous,  $\mathcal{E}_{\delta_1, \delta_2}$  is closed; also since  $\mathcal{D}$  is bounded,  $\mathcal{E}_{\delta_1, \delta_2}$  is also bounded. Then we see that both the gradient  $\nabla E$  and the Hessian  $D^2 E$  are continuous on  $\mathcal{E}_{\delta_1, \delta_2}$ , and so we may define

$$C_1 := \sup_{\mathbf{r} \in \mathcal{E}_{\delta_1, \delta_2}} \|\nabla E(\mathbf{r})\|, \quad C_2 := \sup_{\mathbf{r} \in \mathcal{E}_{\delta_1, \delta_2}} \|D^2 E(\mathbf{r})\|,$$

which are both finite, where  $\|\cdot\|$  for the Hessian is the operator norm associated with the Euclidean norm.

**Theorem.** *Let  $t > 0$  and  $s \mapsto (\mathbf{r}(s), \mathbf{p}(s))$  be the solution to (7) for  $s \in [0, t]$ , and suppose that the solution is contained in  $\mathcal{E}_{\delta_1, \delta_2}$ , that is,  $(\mathbf{r}(s), \mathbf{p}(s)) \in \mathcal{E}_{\delta_1, \delta_2}$  for every  $s \in [0, t]$  for some  $\delta_1 \in (0, 1)$  and  $\delta_2 > 0$ . If  $(\mathbf{r}(0), \mathbf{p}(0)) \in \mathcal{K}$ , then the deviation  $\|\mathbf{g}(t)\|$  is bounded as follows:*

$$\|\mathbf{g}(t)\| \leq \varepsilon C_1 e^{C_2 t/2}.$$

*Proof.* Let us introduce the shorthands

$$\mathbf{f}_j(s) := \nabla_j E(\mathbf{r}(s)), \quad \mathbf{f}(s) := \begin{bmatrix} \mathbf{f}_1(s) \\ \vdots \\ \mathbf{f}_N(s) \end{bmatrix} = \nabla E(\mathbf{r}(s)) \in \mathbb{R}^{2N}$$

for brevity. Then we may rewrite the massive equations (7) as

$$\varepsilon \dot{\mathbf{r}}_j(s) = \mathbf{g}_j(s), \quad \varepsilon \dot{\mathbf{p}}_j(s) = -q_j J \mathbf{g}_j(s) - \varepsilon \mathbf{f}_j(s),$$

which yields

$$\dot{\mathbf{g}}_j(s) = -\frac{2q_j}{\varepsilon} J \mathbf{g}_j(s) - \mathbf{f}_j(s)$$

Defining

$$A_j(s) := \exp\left(t \frac{2q_j}{\varepsilon} J\right) = \begin{bmatrix} \cos(2q_j t/\varepsilon) & \sin(2q_j t/\varepsilon) \\ -\sin(2q_j t/\varepsilon) & \cos(2q_j t/\varepsilon) \end{bmatrix}, \quad (20)$$

we have

$$\frac{d}{ds}(A_j(s) \mathbf{g}_j(s)) = -A_j(s) \mathbf{f}_j(s),$$

and integrating both sides on  $[0, t]$ ,

$$\mathbf{g}_j(t) = A_j(-t) \left( \mathbf{g}_j(0) - \int_0^t A_j(s) \mathbf{f}_j(s) ds \right)$$

However, integration by parts of the integral on the right-hand side yields

$$\begin{aligned} \int_0^t A_j(s) \mathbf{f}_j(s) ds &= \frac{\varepsilon}{2q_j} J^{-1} A_j(s) \mathbf{f}_j(s) \Big|_{s=0}^{s=t} - \frac{\varepsilon}{2q_j} J^{-1} \int_0^t A_j(s) \dot{\mathbf{f}}_j(s) ds \\ &= \frac{\varepsilon}{2q_j} J^{-1} \left( A_j(t) \mathbf{f}_j(t) - \mathbf{f}_j(0) \right) - \frac{\varepsilon}{2q_j} J^{-1} \int_0^t A_j(s) D_{jk}^2 E(\mathbf{r}(s)) \dot{\mathbf{r}}_k(s) ds \\ &= -\varepsilon \frac{q_j}{2} J \left( A_j(t) \mathbf{f}_j(t) - \mathbf{f}_j(0) \right) + \frac{q_j}{2} J \int_0^t A_j(s) F_{jk}(s) \mathbf{g}_k(s) ds \end{aligned}$$

where we note that  $q_j^{-1} = q_j$  because  $q_j = \pm 1$ , and also that  $J^{-1} = -J$ ; we also defined  $F_{jk}(s)$ —for each pair  $(j, k)$  with  $1 \leq j, k \leq N$  and every  $s \geq 0$ —as the following  $2 \times 2$  matrix:

$$F_{jk}(s) := D_{jk}^2 E(\mathbf{r}(s)) \quad \text{with} \quad D_{jk}^2 E := \begin{bmatrix} \frac{\partial^2 E}{\partial x_j \partial x_k} & \frac{\partial^2 E}{\partial x_j \partial y_k} \\ \frac{\partial^2 E}{\partial y_j \partial x_k} & \frac{\partial^2 E}{\partial y_j \partial y_k} \end{bmatrix}.$$

Therefore, we have

$$\begin{aligned} \mathbf{g}_j(t) &= A_j(-t) \mathbf{g}_j(0) + \varepsilon \frac{q_j}{2} J \left( \mathbf{f}_j(t) - A_j(-t) \mathbf{f}_j(0) \right) \\ &\quad - \frac{q_j}{2} J A_j(-t) \int_0^t A_j(s) F_{jk}(s) \mathbf{g}_k(s) ds, \end{aligned}$$

where we used the fact that  $A_j(-t)$  and  $J$  commute. Combining these for  $1 \leq j \leq N$ , we have

$$\mathbf{g}(t) = A(-t) \mathbf{g}(0) + \frac{\varepsilon}{2} \mathcal{J} \left( \mathbf{f}(t) - A(-t) \mathbf{f}(0) \right) - \frac{1}{2} \mathcal{J} A(-t) \int_0^t A(s) F(s) \mathbf{g}(s) ds \quad (21)$$

where  $A(s)$  and  $\mathcal{J}$  are  $2N \times 2N$  the block diagonal matrices defined as

$$A(s) := \begin{bmatrix} A_1(s) & & 0 \\ & \ddots & \\ 0 & & A_N(s) \end{bmatrix}, \quad \mathcal{J} := \begin{bmatrix} q_1 J & & 0 \\ & \ddots & \\ 0 & & q_N J \end{bmatrix},$$

and  $F(s)$  is the  $2N \times 2N$  matrix defined as follows:

$$F(s) := \begin{bmatrix} F_{11}(s) & \cdots & F_{1N}(s) \\ \vdots & \ddots & \vdots \\ F_{N1}(s) & \cdots & F_{NN}(s) \end{bmatrix} = \begin{bmatrix} D_{11}^2 E(\mathbf{r}(s)) & \cdots & D_{1N}^2 E(\mathbf{r}(s)) \\ \vdots & \ddots & \vdots \\ D_{N1}^2 E(\mathbf{r}(s)) & \cdots & D_{NN}^2 E(\mathbf{r}(s)) \end{bmatrix} = D^2 E(\mathbf{r}(s)).$$

One easily sees that  $\|A(s)\| = 1$  for every  $s \in \mathbb{R}$  because it follows from (20) that  $\|A_j(s)\| = 1$  for each  $j$ . It is also clear from the definition of  $J$  from (6) that  $\|\mathcal{J}\| = 1$  as well. Furthermore, the assumptions imply that

$$\|f(s)\| = \|\nabla E(\mathbf{r}(s))\| \leq C_1, \quad \|F(s)\| = \|D^2 E(\mathbf{r}(s))\| \leq C_2 \quad \forall s \in [0, t].$$

Therefore, taking the norm of both sides of (21), we obtain

$$\begin{aligned} \|\mathbf{g}(t)\| &\leq \|\mathbf{g}(0)\| + \frac{\varepsilon}{2} \left( \|\mathbf{f}(t)\| + \|\mathbf{f}(0)\| \right) + \frac{1}{2} \int_0^t \|F(s)\| \|\mathbf{g}(s)\| ds \\ &\leq \|\mathbf{g}(0)\| + \varepsilon C_1 + \frac{C_2}{2} \int_0^t \|\mathbf{g}(s)\| ds. \end{aligned} \tag{22}$$

Therefore, by Gronwall's inequality [25], we obtain

$$\|\mathbf{g}(t)\| \leq (\|\mathbf{g}(0)\| + \varepsilon C_1) e^{C_2 t/2}.$$

The claim then follows because  $\mathbf{g}(0) = 0$  due to the assumption that  $(\mathbf{r}(0), \mathbf{p}(0)) \in \mathcal{K}$ .  $\square$

## 5 First-Order Correction to Kinematic Approximation

We have seen that the massless dynamics gives the 0th-order approximation of the massive equation on  $\mathcal{K}$ . In this section, we shall derive the 1st-order correction to the massless dynamics that improves the approximation, albeit for a short time.

### 5.1 First-Order Correction

Let us consider the asymptotic expansion

$$\mathbf{r}_j = \mathbf{r}_j^{(0)} + \varepsilon \mathbf{r}_j^{(1)} + \cdots.$$

Substituting this into (8) gives

$$2q_j J \dot{\mathbf{r}}_j^{(0)} + \varepsilon \left( \ddot{\mathbf{r}}_j^{(0)} + 2q_j J \dot{\mathbf{r}}_j^{(1)} \right) + O(\varepsilon^2) = -\nabla_j E \left( \mathbf{r}^{(0)} + \varepsilon \mathbf{r}^{(1)} + \cdots \right).$$

However, on the right-hand side, we have

$$\nabla_j E \left( \mathbf{r}^{(0)} + \varepsilon \mathbf{r}^{(1)} + \cdots \right) = \nabla_j E(\mathbf{r}^{(0)}) + \varepsilon D_{jk}^2 E(\mathbf{r}^{(0)}) \mathbf{r}_k^{(1)} + O(\varepsilon^2).$$

Thus, equating the  $O(1)$  and  $O(\varepsilon)$  terms gives

$$2q_j J \dot{\mathbf{r}}_j^{(0)} = -\nabla_j E(\mathbf{r}^{(0)}), \quad \ddot{\mathbf{r}}_j^{(0)} + 2q_j J \dot{\mathbf{r}}_j^{(1)} = -D_{jk}^2 E(\mathbf{r}^{(0)}) \mathbf{r}_k^{(1)},$$

that is,  $\mathbf{r}^{(0)}$  satisfies the Kirchhoff equations (9). One may get rid of the time derivatives of  $\mathbf{r}^{(0)}$  from the second equation for  $\mathbf{r}^{(1)}$  as follows: The second equation gives

$$-\frac{q_j}{2}J\ddot{\mathbf{r}}_j^{(0)} + \dot{\mathbf{r}}_j^{(1)} = \frac{q_j}{2}JD_{jk}^2E(\mathbf{r}^{(0)})\mathbf{r}_k^{(1)},$$

whereas, the time-derivative of the first equation gives

$$2q_jJ\ddot{\mathbf{r}}_j^{(0)} = -D_{jk}^2E(\mathbf{r}^{(0)})\dot{\mathbf{r}}_k^{(0)} \implies \frac{q_j}{2}J\ddot{\mathbf{r}}_j^{(0)} = -\frac{1}{4}D_{jk}^2E(\mathbf{r}^{(0)})\dot{\mathbf{r}}_k^{(0)}.$$

We may get rid of  $\dot{\mathbf{r}}^{(0)}$  from the above equation using  $\dot{\mathbf{r}}_k^{(0)} = \frac{q_k}{2}J\nabla_kE(\mathbf{r}^{(0)})$  as follows:

$$\frac{q_j}{2}J\ddot{\mathbf{r}}_j^{(0)} = -\frac{q_k}{8}D_{jk}^2E(\mathbf{r}^{(0)})J\nabla_kE(\mathbf{r}^{(0)}).$$

As a result, we obtain

$$\dot{\mathbf{r}}_j^{(1)} = \frac{q_j}{2}JD_{jk}^2E(\mathbf{r}^{(0)})\mathbf{r}_k^{(1)} - \frac{q_k}{8}D_{jk}^2E(\mathbf{r}^{(0)})J\nabla_kE(\mathbf{r}^{(0)}). \quad (23)$$

## 5.2 Numerical Results: Effect of Correction to Massless Solutions

Figures 8 and 9 show the time evolution of massless solutions  $\mathbf{r}^{(0)}(t)$  (solution of the Kirchhoff equation (9)) and  $\mathbf{r}^{(0)}(t) + \varepsilon\mathbf{r}^{(1)}(t)$  (with correction  $\mathbf{r}^{(1)}(t)$  from (23)); both are compared to the massive solution. The parameters and the initial conditions are the same ones (18) as before, and the initial condition for the correction  $\mathbf{r}^{(1)}(t)$  is  $\mathbf{r}^{(1)}(0) = 0$ .

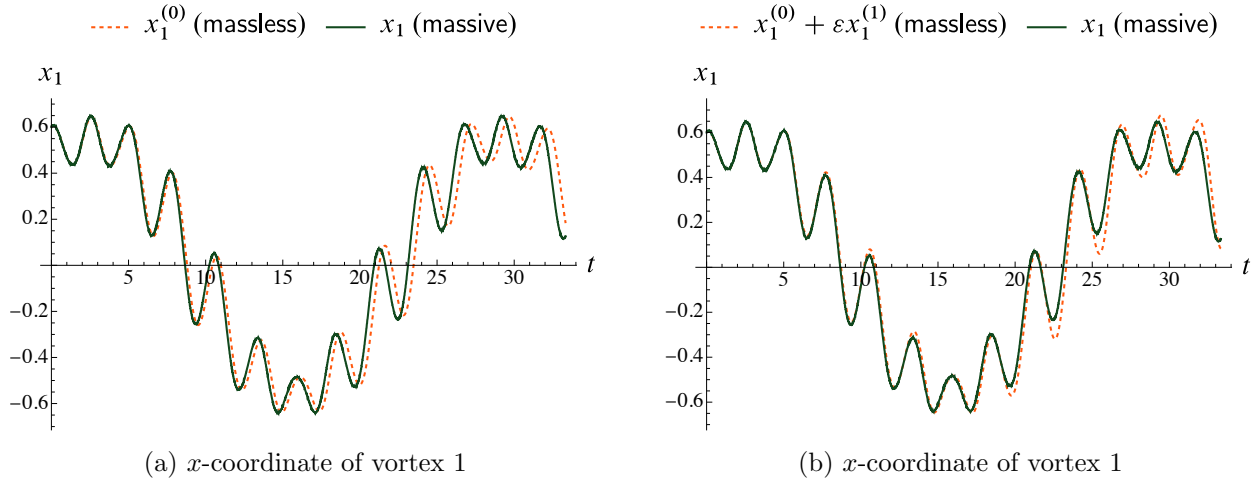


Figure 8: Massless solutions  $x_1^{(0)}(t)$  (without correction) and  $x_1^{(0)}(t) + \varepsilon x_1^{(1)}(t)$  (with correction) of vortex 1, both compared to the massive solution  $x_1(t)$ . The parameter and initial condition are the same as in Figure 3.

The results show that the correction indeed improves the accuracy of the massless solution compared to the massive solution. However, its effect is rather short-lived: It seems to correct the slight time delay of the massless solution  $\mathbf{r}^{(0)}$  but, after a while, the correction exacerbates the massless solution by over-correcting it. This is due to the exponential growth of  $\mathbf{r}^{(1)}(t)$ : The homogeneous part of (23) is a linear Hamiltonian system, and thus it is usually the case that its solutions have some components with exponential growth. Therefore, it is inevitable that the 1st-order correction is viable only for a short time.



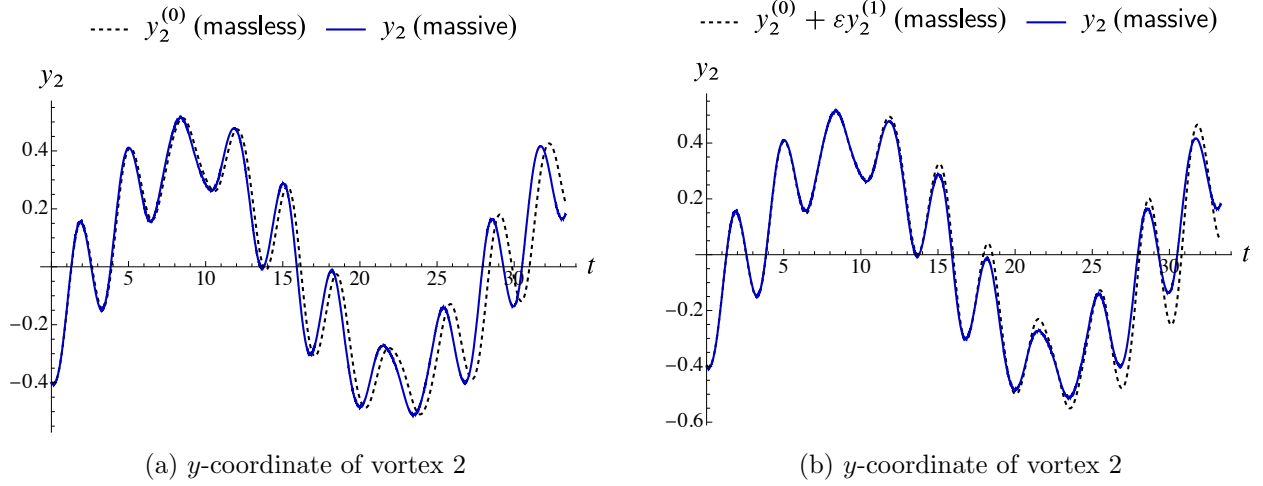


Figure 9: Massless solutions  $y_2^{(0)}(t)$  (without correction) and  $y_2^{(0)}(t) + \epsilon y_2^{(1)}(t)$  (with correction) of vortex 1, both compared to the massive solution  $y_2(t)$ . The parameter and initial condition are the same as in Figure 4.

## 6 Initial Layer Asymptotics

### 6.1 Initial Layers

So far, we have compared massless solutions with massive ones with its initial point  $(\mathbf{r}(0), \mathbf{p}(0))$  lying in the kinematic subspace  $\mathcal{K}$ . The numerical results from Sections 3.5 and 5.2 show that the massless solutions indeed give very good approximations to the massive solution as long as  $(\mathbf{r}(0), \mathbf{p}(0)) \in \mathcal{K}$ .

What happens if the initial condition is not on  $\mathcal{K}$ ? To see this, we consider the initial condition with the same  $\mathbf{r}(0)$  from (18):

$$\mathbf{r}_1(0) = \begin{bmatrix} 0.6 \\ 0.2 \end{bmatrix}, \quad \mathbf{r}_2(0) = \begin{bmatrix} -0.3 \\ -0.4 \end{bmatrix}, \quad (24a)$$

but with the following slightly perturbed initial momenta  $\mathbf{p}(0)$

$$\mathbf{p}_j(0) = q_j J \mathbf{r}_j(0) + \delta \mathbf{p}_j \quad \text{with} \quad \delta \mathbf{p}_1 = \begin{bmatrix} -0.03 \\ 0.025 \end{bmatrix} \quad \text{and} \quad \delta \mathbf{p}_2 = \begin{bmatrix} 0.015 \\ -0.04 \end{bmatrix} \quad (24b)$$

for the massive equations (7). We assume the same initial condition on  $\mathbf{r}^{(0)}$  for the massless solutions as well (hence the same solution as before):

$$\mathbf{r}_j^{(0)}(0) = \mathbf{r}_j(0).$$

Figure 10 shows the time evolution of the  $x$ -coordinate of vortex 1 for the massless and massive solutions. Note that the massless solution is the same as Figures 3 and 8a because we have not changed the initial positions  $\mathbf{r}(0)$ . In particular, Figure 10a shows how the small perturbation in  $\mathbf{p}(0)$  changed the massive solution from Figure 8a considerably: It resulted in a significant deviation from the massless solution.

The massive solution also exhibits small but more noticeable fast oscillations; see Figure 10b for the initial layer of the same solution for  $0 \leq t \leq 0.5$ . The massive solution oscillates very fast, while

the massless solution shows no such oscillations and deviates from the initial layer of the massive solution. This difference in the initial behaviors seems to have resulted in the significant deviation at later times.

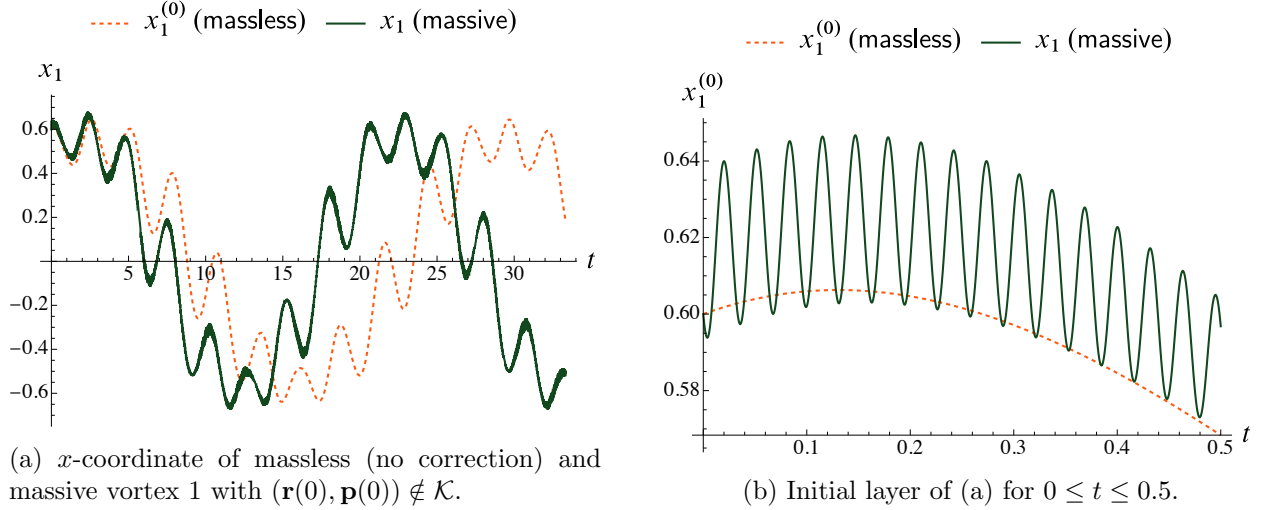


Figure 10: Massless solutions  $x_1^{(0)}(t)$  (without correction) and massive solution  $x_1(t)$  with  $(\mathbf{r}(0), \mathbf{p}(0)) \notin \mathcal{K}$ . The parameter and initial condition are as in (24)—same as (18) except that  $\mathbf{p}(0) = (\mathbf{p}_1(0), \mathbf{p}_2(0))$  is shifted by  $(\delta\mathbf{p}_1, \delta\mathbf{p}_2)$  as shown in (24b).

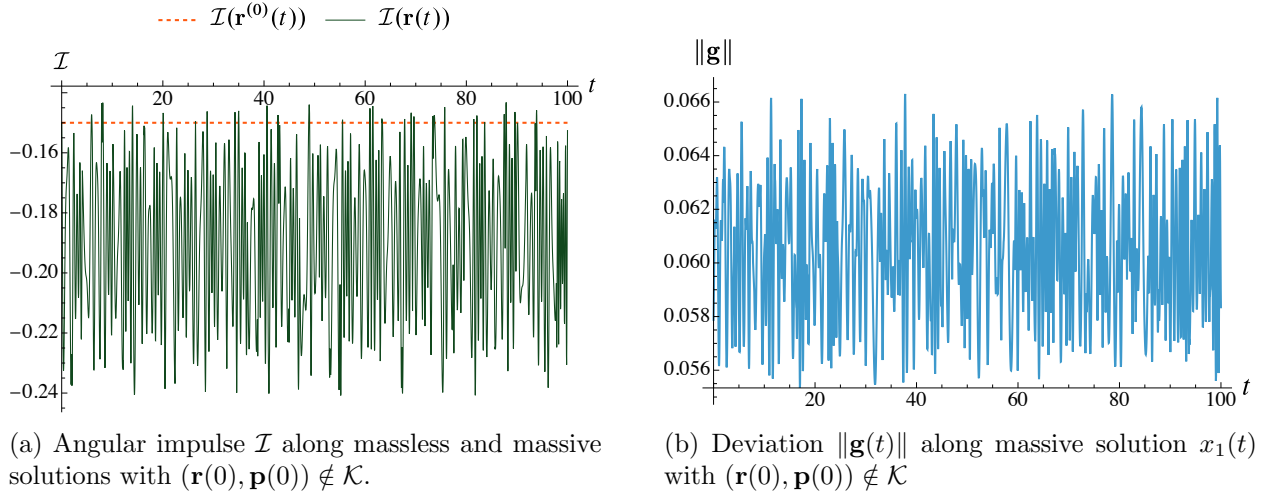


Figure 11: Time evolution of the angular impulse  $\mathcal{I}$  (see (19)) along the massless solution  $\mathbf{r}^{(0)}(t)$  and massive solution  $\mathbf{r}(t)$  with parameters and initial conditions from (24) with  $(\mathbf{r}(0), \mathbf{p}(0)) \notin \mathcal{K}$ .

Additionally, Figure 11a shows the time evolution of the angular impulse  $\mathcal{I}$  from (19) along both the massless solution  $\mathbf{r}^{(0)}(t)$  and massive solution  $\mathbf{r}(t)$  with parameters and initial conditions from (24) with  $(\mathbf{r}(0), \mathbf{p}(0)) \notin \mathcal{K}$ . Comparing it with Figure 6, we notice that the fluctuation of  $\mathcal{I}(\mathbf{r}(t))$  and its deviation from the invariant  $\mathcal{I}(\mathbf{r}^{(0)}(t))$  are far greater than those in Figure 6 with  $(\mathbf{r}(0), \mathbf{p}(0)) \in \mathcal{K}$ , despite the small perturbation in the initial condition. This result again suggests that the solution of the massive system deviates significantly from the massless solution outside the kinematic subspace  $\mathcal{K}$ .

Indeed, Figure 11b shows that the initial deviation  $\|\mathbf{g}(0)\| \simeq 0.058$  persists for  $\|\mathbf{g}(t)\|$  with  $t > 0$  as we have seen in our estimate (22).

## 6.2 Initial Layer and Inner Solutions

The initial layer (or the temporal boundary layer) observed in the massive solution in Figure 10b is characteristic of singularly perturbed systems. It is well known in singular perturbation theory that such an initial layer may be captured by the so-called inner expansion; see, e.g., Neu [45, Chapter 3].

Specifically, let us introduce the rescaled time

$$T := \frac{t}{\varepsilon},$$

and consider the asymptotic (inner) expansion of the form

$$\mathbf{r}(t) = \mathbf{R}^{(0)}(t/\varepsilon) + \varepsilon \mathbf{R}^{(1)}(t/\varepsilon) + \cdots, \quad \mathbf{p}(t) = \mathbf{P}^{(0)}(t/\varepsilon) + \varepsilon \mathbf{P}^{(1)}(t/\varepsilon) + \cdots.$$

Substituting them into (7), we obtain

$$\dot{\mathbf{R}}_j^{(0)} + \varepsilon \dot{\mathbf{R}}_j^{(1)} + \cdots = \mathbf{P}_j^{(0)} - q_j J \mathbf{R}_j^{(0)} + \varepsilon (\mathbf{P}_j^{(1)} - q_j J \mathbf{R}_j^{(1)}) + \cdots,$$

and

$$\dot{\mathbf{P}}_j^{(0)} + \varepsilon \dot{\mathbf{P}}_j^{(1)} + \cdots = -q_j J (\mathbf{P}_j^{(0)} - q_j J \mathbf{R}_j^{(0)}) + \varepsilon (-q_j J (\mathbf{P}_j^{(1)} - q_j J \mathbf{R}_j^{(1)}) - \nabla_j E(\mathbf{R}^{(0)})) + \cdots,$$

where  $(\dot{\cdot})$  stands for  $d/dT$  here. Therefore, equating the  $O(1)$  and  $O(\varepsilon)$  terms, we obtain

$$\dot{\mathbf{R}}_j^{(0)} = \mathbf{P}_j^{(0)} - q_j J \mathbf{R}_j^{(0)}, \quad \dot{\mathbf{P}}_j^{(0)} = -q_j J (\mathbf{P}_j^{(0)} - q_j J \mathbf{R}_j^{(0)})$$

as well as

$$\dot{\mathbf{R}}_j^{(1)} = \mathbf{P}_j^{(1)} - q_j J \mathbf{R}_j^{(1)}, \quad \dot{\mathbf{P}}_j^{(1)} = -q_j J (\mathbf{P}_j^{(1)} - q_j J \mathbf{R}_j^{(1)}) - \nabla_j E(\mathbf{R}^{(0)}).$$

One sees that the first one is a simple linear system

$$\frac{d}{dT} \begin{bmatrix} \mathbf{R}_j^{(0)} \\ \mathbf{P}_j^{(0)} \end{bmatrix} = \begin{bmatrix} -q_j J & I \\ -I & -q_j J \end{bmatrix} \begin{bmatrix} \mathbf{R}_j^{(0)} \\ \mathbf{P}_j^{(0)} \end{bmatrix}.$$

Upon noticing that one can write the matrix as the sum of two commuting matrices

$$\begin{bmatrix} -q_j J & I \\ -I & -q_j J \end{bmatrix} = \begin{bmatrix} -q_j J & 0 \\ 0 & -q_j J \end{bmatrix} + \begin{bmatrix} 0 & I \\ -I & 0 \end{bmatrix},$$

we obtain

$$\begin{aligned} W_j(T) &:= \exp\left(T \begin{bmatrix} -q_j J & I \\ -I & -q_j J \end{bmatrix}\right) = \exp\left(T \begin{bmatrix} -q_j J & 0 \\ 0 & -q_j J \end{bmatrix}\right) \exp\left(T \begin{bmatrix} 0 & I \\ -I & 0 \end{bmatrix}\right) \\ &= \begin{bmatrix} R(q_j T) & 0 \\ 0 & R(q_j T) \end{bmatrix} \begin{bmatrix} (\cos T)I & (\sin T)I \\ -(\sin T)I & (\cos T)I \end{bmatrix} \\ &= \begin{bmatrix} \cos T R(q_j T) & \sin T R(q_j T) \\ -\sin T R(q_j T) & \cos T R(q_j T) \end{bmatrix}, \end{aligned}$$

where

$$R(\theta) := \begin{bmatrix} \cos \theta & -\sin \theta \\ \sin \theta & \cos \theta \end{bmatrix}.$$

As a result, we obtain the 0th-order inner solution

$$\begin{bmatrix} \mathbf{R}_j^{(0)}(T) \\ \mathbf{P}_j^{(0)}(T) \end{bmatrix} = W_j(T) \begin{bmatrix} \mathbf{R}_j^{(0)}(0) \\ \mathbf{P}_j^{(0)}(0) \end{bmatrix},$$

and also the 1st-order correction by a quadrature:

$$\begin{aligned} \begin{bmatrix} \mathbf{R}_j^{(1)}(T) \\ \mathbf{P}_j^{(1)}(T) \end{bmatrix} &= W_j(T) \begin{bmatrix} \mathbf{R}_j^{(1)}(0) \\ \mathbf{P}_j^{(1)}(0) \end{bmatrix} - \int_0^T W_j(T-s) \begin{bmatrix} 0 \\ \nabla_j E(\mathbf{R}^{(0)}(s)) \end{bmatrix} ds \\ &= W_j(T) \begin{bmatrix} \mathbf{R}_j^{(1)}(0) \\ \mathbf{P}_j^{(1)}(0) \end{bmatrix} - \int_0^T \begin{bmatrix} \sin(T-s) R(q_j(T-s)) \nabla_j E(\mathbf{R}^{(0)}(s)) \\ \cos(T-s) R(q_j(T-s)) \nabla_j E(\mathbf{R}^{(0)}(s)) \end{bmatrix} ds. \end{aligned}$$

### 6.3 Numerical Results: Inner Approximation

Consider the same initial condition from (24), and let us compare the inner solution

$$\mathbf{R}_j^{(0)}(t/\varepsilon) + \varepsilon \mathbf{R}_j^{(1)}(t/\varepsilon) = \begin{bmatrix} X_j^{(0)}(t/\varepsilon) \\ Y_j^{(0)}(t/\varepsilon) \end{bmatrix} + \varepsilon \begin{bmatrix} X_j^{(1)}(t/\varepsilon) \\ Y_j^{(1)}(t/\varepsilon) \end{bmatrix}$$

with initial conditions

$$\mathbf{R}_j^{(0)}(0) = \mathbf{r}_j(0), \quad \mathbf{P}_j^{(0)}(0) = \mathbf{p}_j(0), \quad \mathbf{R}_j^{(1)}(0) = \mathbf{P}_j^{(1)}(0) = 0$$

with the massless solution  $\mathbf{r}^{(0)}(t)$  and the massive solution  $(\mathbf{r}(t), \mathbf{p}(t))$ .

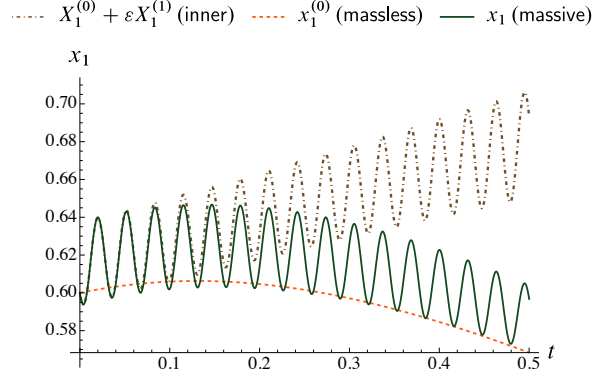
Figures 12 and 13 show the comparison of the inner solution  $\mathbf{R}_j^{(0)}(t/\varepsilon) + \varepsilon \mathbf{R}_j^{(1)}(t/\varepsilon)$ , massless solutions  $\mathbf{r}_j^{(0)}(t)$ , and massive solution  $\mathbf{r}_j(t)$  for both vortices 1 and 2 ( $j = 1, 2$ ). We observe that the inner solution captures the initial layer of the massive solution very well for a short time, but starts deviating from the massive solution later. On the other hand, the massless solution, although missing the small oscillations entirely as mentioned above, behaves roughly like an average of the massive solution. Note, however, that the massless solution also eventually deviates significantly from the massive solution as seen in Figure 10a.

## Conclusions

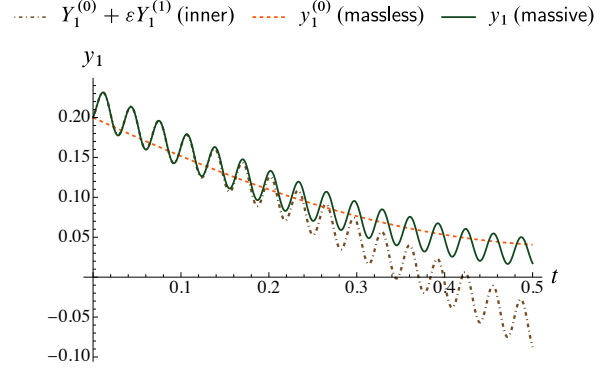
In this work, we analyzed the dynamics of massive point vortices in immiscible Bose–Einstein condensates in the small core mass limit  $\varepsilon \rightarrow 0$ . We showed that the well-known Kirchhoff equations governing massless vortex dynamics emerge as the leading-order approximation to the massive equations, and we derived the first-order correction to this approximation.

Our key findings are:

- (i) The identification of a subspace  $\mathcal{K}$  in the phase space of the massive dynamics such that the massive dynamics starting on  $\mathcal{K}$  stay  $O(\varepsilon)$ -close to the massless dynamics for short times;
- (ii) a rigorous proof of this near-massless behavior of the massive dynamics;

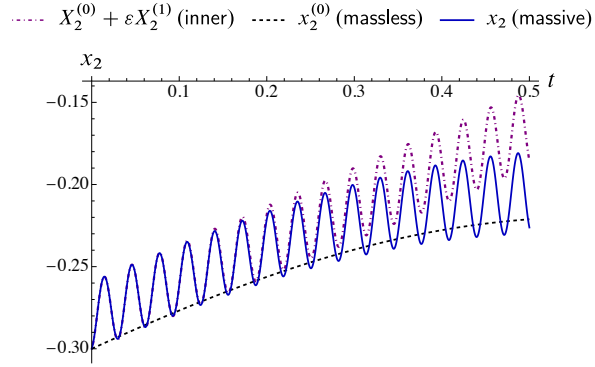


(a)  $x$ -coordinate of inner solution and massive solution of vortex 1

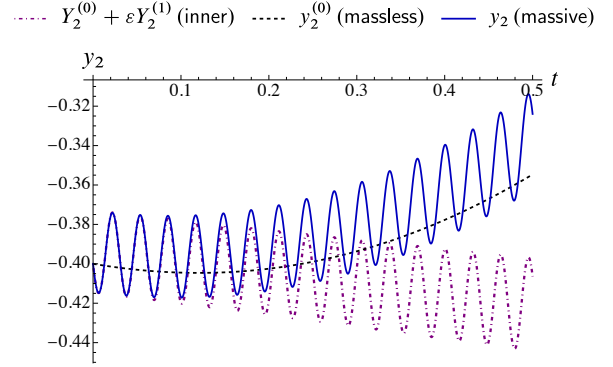


(b)  $y$ -coordinate of inner solution and massive solution of vortex 1

Figure 12: Inner solution  $\mathbf{R}_1^{(0)}(t/\varepsilon) + \varepsilon \mathbf{R}_1^{(1)}(t/\varepsilon)$ , massless solutions  $\mathbf{r}_1^{(0)}(t)$ , and massive solution  $\mathbf{r}_1(t)$  with  $(\mathbf{r}(0), \mathbf{p}(0)) \notin \mathcal{K}$ . The parameter and initial condition are the same as in Figure 10.



(a)  $x$ -coordinate of inner solution and massive solution of vortex 2



(b)  $y$ -coordinate of inner solution and massive solution of vortex 2

Figure 13: Inner solution  $\mathbf{R}_2^{(0)}(t/\varepsilon) + \varepsilon \mathbf{R}_2^{(1)}(t/\varepsilon)$ , massless solutions  $\mathbf{r}_2^{(0)}(t)$ , and massive solution  $\mathbf{r}_2(t)$  with  $(\mathbf{r}(0), \mathbf{p}(0)) \notin \mathcal{K}$ . The parameter and initial condition are the same as in Figure 10.

- (iii) asymptotic analysis of the oscillatory initial layer, a phenomenon typical of singularly perturbed systems, which in our case arises from the presence of a small but vortex mass  $\varepsilon$ .

From a physical perspective, our results are particularly relevant to many experimental systems because vortices acquire an effective inertial mass  $\varepsilon$  due to their tendency to trap particles (tracers, impurities, quantum and thermal excitations, etc). As a result, the conventional massless point-vortex model overlooks an important feature of real systems. By systematically analyzing the asymptotic behaviors as  $\varepsilon \rightarrow 0$ , our work provides a more realistic and physically meaningful description of vortex motion in quantum fluids and is expected to provide a better understanding of various recent and ongoing experiments [27, 34, 44, 51].

This study suggests several directions for future research. One important extension is to explore the vortex dynamics beyond the leading-order approximations, incorporating higher-order corrections to further refine the effective equations of motion. Another promising avenue is a more detailed investigation of the so-called *plasma-orbit theory*, which describes vortex trajectories through an analogy with the motion of charged particles in an external electromagnetic field; see [9, 49]. While the presented analysis has primarily focused on the initial layer, characterizing the short-time initial behavior of solutions, plasma orbit theory appears to be more concerned with the long-time vortex dynamics. A systematic comparison between these two approaches could yield valuable insights into how inertial effects shape vortex motion over different timescales. Expected applications of this improved and more accurate theoretical framework include the instabilities of many-vortex systems [10, 27, 61] and of multiply quantized vortices [17], the formation [65] and sudden rearrangements of vortex crystals [11, 16, 48], the normal modes of vortex necklaces [4, 9, 10, 13, 27], as well as the interaction of vortices in inhomogeneous media [59] and curved substrates [12], or their interplay with other nonlinear excitations [21, 63].

## Acknowledgments

T.O. was supported by NSF grant DMS-2006736. A.R. received funding from the European Union's Horizon research and innovation programme under the Marie Skłodowska-Curie grant agreement *Vortexons* (no. 101062887). A.R. further acknowledges support by the Spanish Ministerio de Ciencia e Innovación (MCIN/AEI/10.13039/501100011033, grant PID2023-147469NB-C21), by the Generalitat de Catalunya (grant 2021 SGR 01411), and by the ICREA *Academia* program. A.R. is grateful to Pietro Massignan for helpful discussions.

## References

- [1] Y.-P. An and L. Li. (In)stability of symbiotic vortex-bright soliton in holographic immiscible binary superfluids. *Journal of High Energy Physics*, 2025(2):42, 2025.
- [2] Y. An and L. Li. Splitting dynamics of quantized composite vortices in holographic miscible binary superfluids. *arXiv preprint arXiv:2501.03561*, 2025.
- [3] F. Ancilotto and L. Reatto. Controlling quantum vortex dynamics and vortex-antivortex annihilation in bose-einstein condensates with optical lattices. *Phys. Rev. A*, 110:013302, Jul 2024. URL <https://link.aps.org/doi/10.1103/PhysRevA.110.013302>.
- [4] P. Banger, Rajat, and S. Gautam. Excitations of a supersolid annular stripe phase in a spin-orbital-angular-momentum-coupled spin-1 bose-einstein condensate. *Phys. Rev. A*, 111:023311, Feb 2025. URL <https://link.aps.org/doi/10.1103/PhysRevA.111.023311>.

- [5] C. Baroni, G. Lamporesi, and M. Zaccanti. Quantum mixtures of ultracold gases of neutral atoms. *Nature Reviews Physics*, 6:736, 2024.
- [6] A. Barresi, A. Boulet, P. Magierski, and G. Wlazłowski. Dissipative dynamics of quantum vortices in fermionic superfluid. *Phys. Rev. Lett.*, 130:043001, Jan 2023. URL <https://link.aps.org/doi/10.1103/PhysRevLett.130.043001>.
- [7] G. P. Bewley, D. P. Lathrop, and K. R. Sreenivasan. Visualization of quantized vortices. *Nature*, 441(7093):588–588, 2006. URL <https://doi.org/10.1038/441588a>.
- [8] G. Boffetta, A. Celani, and P. Franzese. Trapping of passive tracers in a point vortex system. *Journal of Physics A: Mathematical and General*, 29(14):3749, 1996.
- [9] M. Caldara, A. Richaud, M. Capone, and P. Massignan. Massive superfluid vortices and vortex necklaces on a planar annulus. *SciPost Phys.*, 15:057, 2023. URL <https://scipost.org/10.21468/SciPostPhys.15.2.057>.
- [10] M. Caldara, A. Richaud, M. Capone, and P. Massignan. Suppression of the superfluid kelvin-helmholtz instability due to massive vortex cores, friction and confinement. *SciPost Physics*, 17(3):076, 2024.
- [11] L. J. Campbell and R. M. Ziff. Vortex patterns and energies in a rotating superfluid. *Phys. Rev. B*, 20:1886–1902, Sep 1979. URL <https://link.aps.org/doi/10.1103/PhysRevB.20.1886>.
- [12] M. A. Caracanhas, P. Massignan, and A. L. Fetter. Superfluid vortex dynamics on an ellipsoid and other surfaces of revolution. *Phys. Rev. A*, 105:023307, Feb 2022. URL <https://link.aps.org/doi/10.1103/PhysRevA.105.023307>.
- [13] A. Chaika, A. Richaud, and A. Yakimenko. Making ghost vortices visible in two-component bose-einstein condensates. *Phys. Rev. Res.*, 5:023109, May 2023. URL <https://link.aps.org/doi/10.1103/PhysRevResearch.5.023109>.
- [14] S. Choudhury and J. Brand. Rotational pendulum dynamics of a vortex molecule in a channel geometry. *Phys. Rev. A*, 106:043319, Oct 2022. URL <https://link.aps.org/doi/10.1103/PhysRevA.106.043319>.
- [15] S. Choudhury and J. Brand. Distributed vorticity model for vortex molecule dynamics. *Phys. Rev. A*, 107:053314, May 2023. URL <https://link.aps.org/doi/10.1103/PhysRevA.107.053314>.
- [16] I. Coddington, P. C. Haljan, P. Engels, V. Schweikhard, S. Tung, and E. A. Cornell. Experimental studies of equilibrium vortex properties in a Bose-condensed gas. *Phys. Rev. A*, 70:063607, Dec 2004. URL <https://link.aps.org/doi/10.1103/PhysRevA.70.063607>.
- [17] G. Cuomo, Z. Komargodski, and S. Zhong. Chiral modes of giant superfluid vortices. *Phys. Rev. B*, 110:144514, Oct 2024. URL <https://link.aps.org/doi/10.1103/PhysRevB.110.144514>.
- [18] J. D’Ambroise, W. Wang, C. Ticknor, R. Carretero-González, and P. G. Kevrekidis. Stability and dynamics of massive vortices in two-component bose-einstein condensates. *Phys. Rev. E*, 111:034216, Mar 2025. URL <https://link.aps.org/doi/10.1103/PhysRevE.111.034216>.
- [19] P. A. M. Dirac. Note on exchange phenomena in the Thomas atom. *Mathematical Proceedings of the Cambridge Philosophical Society*, 26(03):376–385, 1930.

- [20] R. Doran, A. W. Baggaley, and N. G. Parker. Vortex solutions in a binary immiscible bose-einstein condensate. *Phys. Rev. A*, 109:023318, Feb 2024. URL <https://link.aps.org/doi/10.1103/PhysRevA.109.023318>.
- [21] M. Edmonds. Dark quantum droplets and solitary waves in beyond-mean-field bose-einstein condensate mixtures. *Phys. Rev. Res.*, 5:023175, Jun 2023. URL <https://link.aps.org/doi/10.1103/PhysRevResearch.5.023175>.
- [22] J. Frenkel. *Wave Mechanics: Advanced General Theory*. International series of monographs on physics. Clarendon Press, 1934.
- [23] A. Griffin, V. Shukla, M.-E. Brachet, and S. Nazarenko. Magnus-force model for active particles trapped on superfluid vortices. *Phys. Rev. A*, 101:053601, May 2020. URL <https://link.aps.org/doi/10.1103/PhysRevA.101.053601>.
- [24] A. Griffin, T. Nikuni, and E. Zaremba. *Bose-condensed gases at finite temperatures*. Cambridge University Press, 2009.
- [25] T. H. Gronwall. Note on the derivatives with respect to a parameter of the solutions of a system of differential equations. *Annals of Mathematics*, 20(4):292–296, 1919.
- [26] Y. He and C.-C. Chien. Vortex structure and spectrum of an atomic fermi superfluid in a spherical bubble trap. *Phys. Rev. A*, 108:053303, Nov 2023. URL <https://link.aps.org/doi/10.1103/PhysRevA.108.053303>.
- [27] D. Hernandez-Rajkov, N. Grani, F. Scazza, G. D. Pace, W. J. Kwon, M. Inguscio, K. Xhani, C. Fort, M. Modugno, F. Marino, and G. Roati. Connecting shear flow and vortex array instabilities in annular atomic superfluids. *Nature Physics*, 20:939, 2024. doi: 10.1038/s41567-024-02466-4.
- [28] A. Kanjo and H. Takeuchi. Universal description of massive point vortices and verification methods of vortex inertia in superfluids. *Phys. Rev. A*, 110:063311, Dec 2024. URL <https://link.aps.org/doi/10.1103/PhysRevA.110.063311>.
- [29] G. C. Katsimiga, S. I. Mistakidis, K. Mukherjee, P. G. Kevrekidis, and P. Schmelcher. Stability and dynamics across magnetic phases of vortex-bright type excitations in spinor bose-einstein condensates. *Phys. Rev. A*, 107:013313, Jan 2023. URL <https://link.aps.org/doi/10.1103/PhysRevA.107.013313>.
- [30] J. Kevorkian and J. Cole. *Multiple Scale and Singular Perturbation Methods*. Applied Mathematical Sciences. Springer New York, 1996. ISBN 9780387942025.
- [31] N. M. Khalifa and H. E. Taha. Vortex dynamics: A variational approach using the principle of least action. *Phys. Rev. Fluids*, 9:034701, Mar 2024. URL <https://link.aps.org/doi/10.1103/PhysRevFluids.9.034701>.
- [32] N. B. Kopnin and V. M. Vinokur. Dynamic vortex mass in clean fermi superfluids and superconductors. *Phys. Rev. Lett.*, 81:3952–3955, Nov 1998. URL <https://link.aps.org/doi/10.1103/PhysRevLett.81.3952>.
- [33] P. Kramer and M. Saraceno. *Geometry of the time-dependent variational principle in quantum mechanics*. Lecture notes in physics. Springer-Verlag, 1981.



- [34] W. J. Kwon, G. Del Pace, K. Xhani, L. Galantucci, A. Muzi Falconi, M. Inguscio, F. Scazza, and G. Roati. Sound emission and annihilations in a programmable quantum vortex collider. *Nature*, 600(7887):64–69, 2021.
- [35] H. Lamb. *Hydrodynamics*, chapter 7. Dover, New York, 6th edition, 1945.
- [36] S. Lan, X. Li, J. Mo, Y. Tian, Y.-K. Yan, P. Yang, and H. Zhang. Splitting of doubly quantized vortices in holographic superfluid of finite temperature. *Journal of High Energy Physics*, 2023 (5):1–17, 2023.
- [37] K. J. H. Law, P. G. Kevrekidis, and L. S. Tuckerman. Stable vortex–bright-soliton structures in two-component bose-einstein condensates. *Phys. Rev. Lett.*, 105:160405, Oct 2010. URL <https://link.aps.org/doi/10.1103/PhysRevLett.105.160405>.
- [38] C. Lin. On the motion of vortices in two dimensions: I. existence of the kirchhoff-routh function. *Proceedings of the National Academy of Sciences*, 27(12):570–575, 1941.
- [39] C. Lubich. On variational approximations in quantum molecular dynamics. *Mathematics of Computation*, 74(250):765–779, 2005. ISSN 0025-5718.
- [40] C. Lubich. *From quantum to classical molecular dynamics: reduced models and numerical analysis*. European Mathematical Society, Zürich, Switzerland, 2008.
- [41] P. Magierski, A. Barresi, A. Makowski, D. Pcał, and G. Wlazłowski. Quantum vortices in fermionic superfluids: from ultracold atoms to neutron stars. *The European Physical Journal A*, 60(9):186, 2024.
- [42] A. D. McLachlan. A variational solution of the time-dependent Schrodinger equation. *Molecular Physics*, 8(1):39–44, 1964.
- [43] Y. Minowa, Y. Yasui, T. Nakagawa, S. Inui, M. Tsubota, and M. Ashida. Direct excitation of kelvin waves on quantized vortices. *Nature Physics*, 21:233, 2025.
- [44] T. W. Neely, G. Gauthier, C. Glasspool, M. J. Davis, and M. T. Reeves. Melting of a vortex matter wigner crystal. *arXiv preprint arXiv:2402.09920*, 2024.
- [45] J. Neu. *Singular Perturbation in the Physical Sciences*. Graduate Studies in Mathematics. American Mathematical Society, 2015.
- [46] R. O’Malley. *Singular Perturbation Methods for Ordinary Differential Equations*. Applied Mathematical Sciences. Springer New York, 1991. ISBN 9783540975564.
- [47] S. Patrick, A. Gupta, R. Gregory, and C. F. Barenghi. Stability of quantized vortices in two-component condensates. *Phys. Rev. Res.*, 5:033201, Sep 2023. URL <https://link.aps.org/doi/10.1103/PhysRevResearch.5.033201>.
- [48] E. Poli, T. Bland, S. J. M. White, M. J. Mark, F. Ferlaino, S. Trabucco, and M. Mannarelli. Glitches in rotating supersolids. *Phys. Rev. Lett.*, 131:223401, Nov 2023. URL <https://link.aps.org/doi/10.1103/PhysRevLett.131.223401>.
- [49] E. Poli, A. Litvinov, E. Casotti, C. Ulm, L. Klaus, M. J. Mark, G. Lamporesi, T. Bland, and F. Ferlaino. Synchronization in rotating supersolids. *arXiv preprint arXiv:2412.11976*, 2024.

- [50] S. B. Prasad, N. G. Parker, and A. W. Baggaley. Vortex-pair dynamics in three-dimensional homogeneous dipolar superfluids. *Phys. Rev. A*, 109:063323, Jun 2024. URL <https://link.aps.org/doi/10.1103/PhysRevA.109.063323>.
- [51] M. T. Reeves, K. Goddard-Lee, G. Gauthier, O. R. Stockdale, H. Salman, T. Edmonds, X. Yu, A. S. Bradley, M. Baker, H. Rubinsztein-Dunlop, M. J. Davis, and T. W. Neely. Turbulent relaxation to equilibrium in a two-dimensional quantum vortex gas. *Phys. Rev. X*, 12:011031, Feb 2022. URL <https://link.aps.org/doi/10.1103/PhysRevX.12.011031>.
- [52] A. Richaud, V. Penna, R. Mayol, and M. Guilleumas. Vortices with massive cores in a binary mixture of Bose-Einstein condensates. *Phys. Rev. A*, 101:013630, 2020.
- [53] A. Richaud, V. Penna, and A. L. Fetter. Dynamics of massive point vortices in a binary mixture of Bose-Einstein condensates. *Phys. Rev. A*, 103:023311, 2021.
- [54] A. Richaud, P. Massignan, V. Penna, and A. L. Fetter. Dynamics of a massive superfluid vortex in  $r^k$  confining potentials. *Phys. Rev. A*, 106:063307, Dec 2022. URL <https://link.aps.org/doi/10.1103/PhysRevA.106.063307>.
- [55] A. Richaud, G. Lamporesi, M. Capone, and A. Recati. Mass-driven vortex collisions in flat superfluids. *Phys. Rev. A*, 107:053317, May 2023. URL <https://link.aps.org/doi/10.1103/PhysRevA.107.053317>.
- [56] A. Richaud, M. Caldara, M. Capone, P. Massignan, and G. Wlazłowski. Dynamical signature of vortex mass in fermi superfluids. *arXiv preprint arXiv:2410.12417*, 2024.
- [57] V. P. Ruban. Direct and reverse precession of a massive vortex in a binary bose-einstein condensate. *JETP Letters*, 115(7):415–421, 2022.
- [58] V. P. Ruban, W. Wang, C. Ticknor, and P. G. Kevrekidis. Instabilities of a vortex-ring-bright soliton in trapped binary three-dimensional bose-einstein condensates. *Phys. Rev. A*, 105:013319, Jan 2022. URL <https://link.aps.org/doi/10.1103/PhysRevA.105.013319>.
- [59] S.-H. Shinn and A. del Campo. Electrodynamics of vortices in quasi-two-dimensional scalar bose-einstein condensates. *Phys. Rev. Res.*, 7:013217, Feb 2025. URL <https://link.aps.org/doi/10.1103/PhysRevResearch.7.013217>.
- [60] E. Šimánek. Reactive effects of core fermion excitations on the inertial mass of a vortex. *Journal of low temperature physics*, 100:1–19, 1995.
- [61] S. Simjanovski, G. Gauthier, H. Rubinsztein-Dunlop, M. T. Reeves, and T. W. Neely. Shear-induced decaying turbulence in bose-einstein condensates. *Phys. Rev. A*, 111:023314, Feb 2025. URL <https://link.aps.org/doi/10.1103/PhysRevA.111.023314>.
- [62] T. Simula. Vortex mass in a superfluid. *Phys. Rev. A*, 97:023609, Feb 2018. URL <https://link.aps.org/doi/10.1103/PhysRevA.97.023609>.
- [63] V. Skogvoll, J. Rønning, M. Salvalaglio, and L. Angheluta. A unified field theory of topological defects and non-linear local excitations. *npj Computational Materials*, 9(1):122, 2023.
- [64] S. Trabucco, L. Lepori, M. L. Chiofalo, and M. Mannarelli. Binary superfluids: low-energy properties and dissipative processes from spontaneous emission of massive phonons. *arXiv preprint arXiv:2501.10194*, 2025.

- [65] S. Tsuzuki, E. Itoh, and K. Nishinari. Three-dimensional analysis of vortex-lattice formation in rotating bose–einstein condensates using smoothed-particle hydrodynamics. *Journal of Physics Communications*, 7(12):121001, 2023.
- [66] A. M. Turner. Mass of a spin vortex in a bose-einstein condensate. *Phys. Rev. Lett.*, 103:080603, Aug 2009. URL <https://link.aps.org/doi/10.1103/PhysRevLett.103.080603>.
- [67] W. Wang. Controlled engineering of a vortex-bright soliton dynamics using a constant driving force. *Journal of Physics B: Atomic, Molecular and Optical Physics*, 55(10):105301, 2022.
- [68] L. A. Williamson and P. B. Blakie. Damped point-vortex model for polar-core spin vortices in a ferromagnetic spin-1 bose-einstein condensate. *Phys. Rev. Res.*, 3:013154, Feb 2021. URL <https://link.aps.org/doi/10.1103/PhysRevResearch.3.013154>.
- [69] S. Yao, Y. Tian, P. Yang, and H. Zhang. Baby skyrmion in two-component holographic superfluids. *Journal of High Energy Physics*, 2023(8):55, 2023.